



Research Article

Algae 2021, 36(4): 263-283
<https://doi.org/10.4490/algae.2021.36.11.28>

Open Access



Ecophysiology of the kleptoplastidic dinoflagellate *Shimiella gracilenta*: I. spatiotemporal distribution in Korean coastal waters and growth and ingestion rates

Jin Hee Ok¹, Hae Jin Jeong^{1,2,*}, Hee Chang Kang¹, Sang Ah Park¹, Se Hee Eom¹, Ji Hyun You¹ and Sung Yeon Lee¹

¹School of Earth and Environmental Sciences, College of Natural Sciences, Seoul National University, Seoul 08826, Korea

²Research Institute of Oceanography, Seoul National University, Seoul 08826, Korea

To explore the ecophysiological characteristics of the kleptoplastidic dinoflagellate *Shimiella gracilenta*, we determined its spatiotemporal distribution in Korean coastal waters and growth and ingestion rates as a function of prey concentration. The abundance of *S. gracilenta* at 28 stations from 2015 to 2018 was measured using quantitative real-time polymerase chain reaction. Cells of *S. gracilenta* were detected at least once at all the stations and in each season, when temperature and salinity were 1.7–26.4°C and 9.9–35.6, respectively. Moreover, among the 28 potential prey species tested, *S. gracilenta* SGJH1904 fed on diverse prey taxa. However, the highest abundance of *S. gracilenta* was only 3 cells mL⁻¹ during the study period. The threshold *Teleaulax amphioxeia* concentration for *S. gracilenta* growth was 5,618 cells mL⁻¹, which was much higher than the highest abundance of *T. amphioxeia* (667 cells mL⁻¹). Thus, *T. amphioxeia* was not likely to support the growth of *S. gracilenta* in the field during the study period. However, the maximum specific growth and ingestion rates of *S. gracilenta* on *T. amphioxeia*, the optimal prey species, were 1.36 d⁻¹ and 0.04 ng C predator⁻¹ d⁻¹, respectively. Thus, if the abundance of *T. amphioxeia* was much higher than 5,618 cells mL⁻¹, the abundance of *S. gracilenta* could be much higher than the highest abundance observed in this study. Eurythermal and euryhaline characteristics of *S. gracilenta* and its ability to feed on diverse prey species and conduct kleptoplastidy are likely to be responsible for its common spatiotemporal distribution.

Key Words: abundance; feeding; *Gymnodinium gracilellum*; Kareniaceae; protist; qPCR

INTRODUCTION

Dinoflagellates are one of the major eukaryotic microorganism groups in marine ecosystems and are ubiquitously present from the equator to the polar (Taylor et al. 2008, Jeong et al. 2021a). They have three major trophic modes: autotrophy, mixotrophy, and heterotrophy (Hansen 1991b, Schnepf and Elbrächter 1992, Jeong et al. 2010a, Stoecker et al. 2017). Thus, they play diverse eco-

logical roles, such as primary producers, prey, predators, symbionts, and parasites (Hansen 1991a, Coats 1999, Stat et al. 2008, Jeong et al. 2010b, Fraga et al. 2012, You et al. 2020). They often dominate protist assemblages and cause red tides or harmful algal blooms (Hallegraeff 1993, Smayda and Reynolds 2003, Jeong et al. 2013, Ok et al. 2021b). Furthermore, phototrophic (autotrophic and



This is an Open Access article distributed under the terms of the Creative Commons Attribution Non-Commercial License (<http://creativecommons.org/licenses/by-nc/3.0/>) which permits unrestricted non-commercial use, distribution, and reproduction in any medium, provided the original work is properly cited.

Received September 17, 2021, Accepted November 28, 2021

*Corresponding Author

E-mail: hjeong@snu.ac.kr

Tel: +82-2-880-6746, Fax: +82-2-874-9695

mixotrophic) dinoflagellates are known to have the largest portion of the annual integrated carbon retention of plankton in Masan Bay, Korea (Jeong et al. 2021b). Therefore, to understand the structure and function of marine ecosystems, the distribution of dinoflagellates in the sea and their ecological roles should be explored.

To predict the distribution of dinoflagellates in the sea, its abundance in different regions and environmental factors affecting the abundance should be determined (Bockstahler and Coats 1993, Li et al. 2000, Jeong et al. 2015, Hernández-Becerril et al. 2018, Lee et al. 2019a, 2019b, Ok et al. 2019, Kang et al. 2020). The distribution of dinoflagellates is affected by diverse abiotic factors, such as water temperature, salinity, and nutrient concentrations (Drira et al. 2008, Cohu et al. 2011, Kang et al. 2019, Lee et al. 2021). Furthermore, biotic factors, such as the abundance of prey, predators, and competitors, affect the distribution of dinoflagellates (Tillmann and Reckermann 2002, Matsubara et al. 2007, Jeong et al. 2015). The distribution of autotrophic dinoflagellates is known to be primarily affected by light, nutrient concentrations, water temperature, and predators (Booth and Smith 1997, Gímez et al. 2011, Jeong et al. 2015, Golubkov et al. 2019), whereas that of heterotrophic dinoflagellates is affected by prey and predators (Verity et al. 1993, Jeong 1999, Jeong et al. 2010b, Kim et al. 2013). The distributions of mixotrophic dinoflagellates are mainly affected by prey, light, nutrient concentrations, water temperature, and predators (Bockstahler and Coats 1993, Smalley and Coats 2002, Baek et al. 2008a, 2008b, Jeong et al. 2013, 2015, Yoo et al. 2013, Ok et al. 2017, Golubkov et al. 2019, Jang and Jeong 2020, Eom et al. 2021). Some heterotrophic dinoflagellates conduct photosynthesis using the plastids of ingested prey and are called kleptoplastidic dinoflagellates (Larsen 1988, Schnepf 1992, Schnepf and Elbrächter 1992, 1999, Skovgaard 1998, Gast et al. 2007, Raven et al. 2009, Johnson 2011, Hehenberger et al. 2019). Previous studies have investigated the distribution of only a few kleptoplastidic dinoflagellates such as *Dinophysis* spp., *Pfiesteria piscicida*, and *Gymnodinium smaydae* (Jeong et al. 2006, Lin et al. 2006, Díaz et al. 2011, Lee et al. 2020). However, the distribution of more kleptoplastidic dinoflagellates, environmental factors affecting their distributions, and eco-evolutionary strategies need to be investigated.

Recently, a kleptoplastidic dinoflagellate, *Shimiella gracilenta*, has been described (Ok et al. 2021a). This dinoflagellate was originally named *Gymnodinium gracilentum* until recently established as *S. gracilenta* based on molecular and electron microscopic analyses (Camp-

bell 1973, Ok et al. 2021a). To date, some ecophysiological characteristics of *S. gracilenta* have been investigated (Skovgaard 1998, Jakobsen et al. 2000, Park et al. 2021); light provided positive effects on the growth and ingestion of *S. gracilenta* under food-repleted conditions using kleptoplastids and enhanced the survival of *S. gracilenta* under food-depleted conditions (Skovgaard 1998); moreover, the growth rate of *S. gracilenta* was saturated at a light intensity of 60–80 µmol photons m⁻² s⁻¹ (Jakobsen et al. 2000). Interactions between *S. gracilenta* and heterotrophic protists have been recently explored. *Shimiella gracilenta* has only a few heterotrophic protistan predators but supports moderate growth rates of the predators (Park et al. 2021). However, spatial and temporal distributions of *S. gracilenta*, abiotic and biotic factors affecting the distribution, and the numerical and functional responses of *S. gracilenta* to prey concentration have not yet been explored.

Cells of *S. gracilenta* are <13 µm in length and fragile due to lack of theca (Ok et al. 2021a). Some dinoflagellates belonging to Gymnodiniales (e.g., *Gymnodinium minutulum* and *Gymnodinium octo*) are morphologically similar to *S. gracilenta* (Campbell 1973, Larsen 1994), making it difficult to distinguish *S. gracilenta* from other dinoflagellate species in fixed samples under light microscopes. Thus, to quantify the abundance of *S. gracilenta*, molecular techniques such as quantitative real-time polymerase chain reaction (qPCR) should be used.

In the present study, the abundance of *S. gracilenta* was quantified at 28 coastal stations along the Korean Peninsula and Jeju Island during four seasons from April 2015 to October 2018, using a qPCR with a newly developed primer-probe set of *S. gracilenta*. Seawaters from the 28 stations have a wide range of water temperatures, salinities, and nutrient concentrations due to the temperate climate and freshwater input from large rivers (Kang et al. 2019, Lee et al. 2019b). Thus, these stations are ideal regions for exploring the environmental factors affecting the distribution of *S. gracilenta*. Correlations between the abundance of *S. gracilenta* and water temperature, salinity, dissolved oxygen (DO), and the concentrations of nutrients and chlorophyll-a (Chl-a) were explored. Furthermore, to investigate the effects of biotic factors on the distribution of *S. gracilenta*, the prey species that *S. gracilenta* is able to feed on and growth and ingestion rates of *S. gracilenta* on suitable prey species as a function of prey concentration were determined. Using the data on the abundance of prey species in the literature (Jang and Jeong 2020) and the data on the abundance of *S. gracilenta* in the present study, the correlations between the

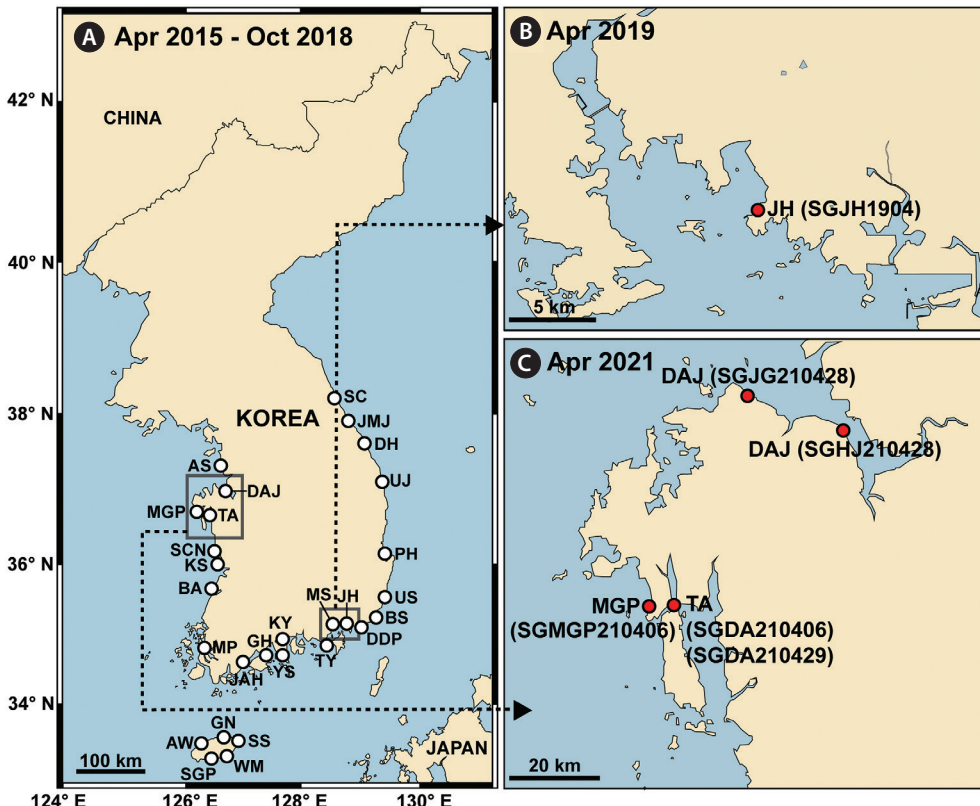


Fig. 1. Map showing the study area. (A) The sampling stations for quantitative real-time polymerase chain reaction during April 2015–October 2018. (B) A site where *Shimiella gracilenta* was isolated in South Sea of Korea in April 2019. (C) Sites where *S. gracilenta* was isolated in West Sea of Korea in April 2021. Names in parenthesis represent the strain names of *S. gracilenta*. SC, Sokcho; JMJ, Jumunjin; DH, Donghae; UJ, Uljin; PH, Pohang; US, Ulsan; BS, Busan; DDP, Dadaepo; MS, Masan; JH, Jinhae; TY, Tongyoung; YS, Yeosu; KY, Kwangyang; GH, Goheung; JAH, Jangheung; AS, Ansan; DAJ, Dangjin; MGP, Mageompo; TA, Taean; SCN, Seocheon; KS, Kunsan; BA, Buan; MP, Mokpo; AW, Aewol; SGP, Seogwipo; WM, Wimi; SS, Seongsan; GN, Gimnyeong.

abundance of *S. gracilenta* and each prey species were explored. The results of the present study provide a basis for understanding the distribution of kleptoplastidic dinoflagellates and biotic and abiotic environmental factors affecting their distribution.

MATERIALS AND METHODS

Field sample collection during 2015–2018

Surface water samples were collected from 28 stations along the Korean Peninsula (East, West, and South Seas) and Jeju Island during 2015–2018 (Fig. 1A). These samples were collected seasonally between April 2015 and October 2018 (Supplementary Table S1).

Data on the water temperature, salinity, DO, Chl-*a* concentration, and the concentration of nitrite plus nitrate ($\text{NO}_2 + \text{NO}_3$, hereafter NO_3), phosphate (PO_4), and

silicate (SiO_2) of seawater at 28 stations during the study period were obtained from our previous studies (Kang et al. 2019, Lee et al. 2019b).

For qPCR analysis, 40–600 mL of seawater was filtered through 25-mm GF/C filters (Whatman Inc., Clifton, NJ, USA). The filtered membrane was stored in a 2.0-mL tube and frozen at -20°C until transfer to the laboratory. DNA from the filtered membrane was extracted using the AcuPrep Genomic DNA Extraction Kit (Bioneer, Daejeon, Korea).

Culture of *Shimiella gracilenta*

Shimiella gracilenta SGJH1904 was isolated from a water sample collected from surface water off Jinhae Bay, Korea, in April 2019, when water temperature and salinity were 14.6°C and 33.6, respectively (Fig. 1B) (Ok et al. 2021a). The clonal culture of this dinoflagellate was established using two consecutive single-cell isolations,

and the cryptophyte *Teleaulax amphioxiae* was provided as prey every 3–4 days (30,000–50,000 cells mL⁻¹). The clonal culture in a 250-mL cell culture flask was placed on a shelf at 20°C under a 14 : 10 h light : dark cycle and 20 µmol photons m⁻² s⁻¹ of cool white fluorescent light.

Species-specific primer and probe design and specificity analysis

To develop a species-specific primer and probe set for *S. gracilenta*, the sequences of the internal transcribed spacer region of ribosomal DNA (ITS rDNA) of *S. gracilenta* SGJH1904 and other dinoflagellate species belonging to the family Kareniaceae and related dinoflagellate species were obtained from GenBank (Supplementary Table S2). These sequences were aligned using MEGA v.4 (Tamura et al. 2007). The unique part of the ITS rDNA sequences for *S. gracilenta* was searched from the alignments to develop the *S. gracilenta*-specific primers and probe. The primer and probe sequences were analyzed using Primer 3 (Whitehead Institute for Biomedical Research, Cambridge, MA, USA) and Oligo Calc: Oligonucleotide Properties Calculator (Kibbe 2007) to determine the optimal melting temperature and secondary structure, respectively. The primers and probe were synthesized by Bioneer (Table 1). The probe was dual-labeled with the fluorescent dyes FAM and BHQ1 at the 5' and 3' ends.

Specificity analysis of the primer and probe sets for *S. gracilenta* was conducted using DNA extracts of *S. gracilenta* SGJH1904, 24 dinoflagellate species in Gymnodiniales, Amphidiniales, Dinophysales, Peridiniales, Suessiales, and Thoracosphaerales and cryptophycean prey *T. amphioxiae* (Supplementary Table S3).

The qPCR reaction mixture contained 1 µL of DNA template, 0.2 µM of specific forward and reverse primers, 0.15 µM of the specific probe, 5 µL of qPCR Bio Probe Separate-ROX (Genepole, Gwangmyeong, Korea), and deionized sterilized water (DDW; Bioneer), with a final total volume of 10 µL. The qPCR assay was performed us-

ing the Rotor-Gene Q (Qiagen, Hilden, Germany). The cycling conditions were initialized with a denaturation step at 95°C for 3 min, followed by 40 cycles of 10 s at 95°C for 10 s, and 58°C for 40 s.

Standard curve construction

A standard curve for determining the abundance of *S. gracilenta* was constructed using a qPCR. DNA was extracted from the culture of *S. gracilenta* SGJH1904 (104,000 cells mL⁻¹) in the growth phase using the Accu-Prep Genomic DNA Extraction Kit (Bioneer), targeting 1, 10, 100, 1,000, 10,000, and 100,000 *S. gracilenta* cells. The qPCR assay was conducted using the reaction mixture mentioned above under the following thermal cycling conditions: 95°C for 3 min, followed by 45 cycles of 10 s at 95°C for 10 s, and 58°C for 40 s.

Quantification using qPCR

DNA samples extracted from seawater were used as the template. Samples using a DDW as the template in the reaction mixture were used as non-template controls. Samples from *S. gracilenta* SGJH1904 as a template were used as positive and standard controls. The method and conditions used for qPCR to determine the abundance of *S. gracilenta* in field samples collected during 2015–2018 were the same as those described in the standard curve construction section.

Confirmation of the presence of *Shimiella gracilenta*

The abundance of *S. gracilenta*, measured using the qPCR method in the present study, was as low as 0.01–3 cells mL⁻¹ at all the stations. Thus, surface water samples were collected from three stations in April 2021 to confirm the presence of *S. gracilenta* cells in the samples (Fig 1C). The aliquots were poured into 50 mL flasks containing *T. amphioxiae* or *Pyramimonas* sp. as prey. The flasks

Table 1. Sequences of the primers and probe for *Shimiella gracilenta* used in this study

Analysis	Primer region	Primer / Probe name	Direction	Sequence (5'-3')	Reference
PCR	ITS-LSU rDNA	ITSF2	Forward	TACGTCCCTGCCCTTGTC	Litaker et al. (2003)
		LSU500R	Reverse	CCCTCATGGTACTTGTTC	
qPCR	ITS rDNA	Sgracilenta_F	Forward	ACGCATTCAAGTTCACAGGTAC	This study
		Sgracilenta_R	Reverse	AGATTCCGAATCAGAGCAGG	
		Sgracilenta_P		[FAM] TCTGTGTACATCGTTGCTTGATGGC [BHQ1]	

ITS, internal transcribed spacer; LSU, large subunit; PCR, polymerase chain reaction; qPCR, quantitative real-time PCR.

were incubated at 20°C under a 14 : 10 h light : dark cycle and 20 µmol photons m⁻² s⁻¹ of cool white fluorescent light for 3–4 days. After incubation, the contents of the flasks were distributed to 96-well plate chambers. When cells of a dinoflagellate similar to *S. gracilenta* were observed in each chamber in 96-well plates, single-cell isolations were conducted. Finally, two strains SGDA210406 and SGDA210429 from Taean, a strain SGMGP210406 from Mageompo, and two strains SGJG210428 and SGHJ210428 from Dangjin were established (Fig. 1C). The ITS rDNA sequences of these five strains were analyzed to confirm whether they were identical to *S. gracilenta* SGJH1904 (GenBank accession No. MN965778).

The 100–200 mL aliquots of the seawater samples were used to quantify the abundance of *S. gracilenta* using qPCR, as described above.

Feeding occurrence and mechanism

To explore the effects of prey species on the distribution of *S. gracilenta*, the prey species that *S. gracilenta* is able to feed on were investigated. Twenty-seven microalgal species and *Mesodinium rubrum* were provided as potential prey items (Supplementary Table S4). All prey species except the haptophyte *Phaeocystis antarctica* and the photosynthetic ciliate *M. rubrum* were grown in enriched f/2 or L1 seawater media under the same temperature and light conditions as described above (Guillard and Ryther 1962, Guillard and Hargraves 1993). *Mesodinium rubrum* cells were grown under the same temperature and light conditions described above, and *T. amphioxiae* was provided as prey. Cells of *P. antarctica* were grown at 5°C under a 14 : 10 h light : dark cycle and 50 µmol photons m⁻² s⁻¹ of cool white fluorescent light in enriched L1 seawater medium. The mean equivalent spherical diameter (ESD) of prey species was obtained from previous studies and literature (Mathot et al. 2000, Jeong et al. 2014, Lee et al. 2016, Lim et al. 2018, Eom et al. 2021). The ESD of *Chrysochromulina* sp. CSYS1905 and

Apedinella sp. ASGY1807 was calculated in this study.

Experiment 1 was conducted to investigate whether *S. gracilenta* SGJH1904 was able to feed on the target prey species (Table 2). Moreover, the feeding mechanism of *S. gracilenta* with regard to the edible prey species was examined. Dense cultures of *S. gracilenta* growing on *T. amphioxiae* were transferred to 800-mL cell culture flasks containing fresh seawater and *T. amphioxiae*. When prey cells were not detectable (ND) in the seawater, 5-mL aliquots were removed from the flasks and the cell concentration of *S. gracilenta* was determined under a compound microscope (BX53; Olympus, Tokyo, Japan).

In this experiment, the initial concentrations of *S. gracilenta* and each target prey species were established by using an autopipette to deliver a predetermined volume of culture to 42-mL polycarbonate (PC) experimental bottles. One 42-mL PC experimental bottle containing mixtures of *S. gracilenta* and a target prey species, one prey-only control bottle, and one *S. gracilenta*-only control bottle were set up. The PC bottles were filled with freshly filtered seawater, capped, placed on a rotating wheel at 0.9 rpm (0.00017 ×g), and incubated under the same conditions as described above. For *P. antarctica*, this experiment was conducted at 10°C because this prey can grow at low temperatures. After 2, 24, and 48 h of incubation, a 5-mL aliquot from each bottle was removed and transferred to a 6-well plate chamber. Cells of *S. gracilenta* were tracked to examine physical contact, attack (attempt to capture), and successful capture (ingestion) using a dissecting microscope at a magnification of 10–63× and an inverted microscope at a magnification of 200–1,000× (Axiovert 200M; Carl Zeiss, Göttingen, Germany). Cells of *S. gracilenta* incubated with each target prey species were photographed at a magnification of 1,000× using an inverted microscope. The feeding mechanism of *S. gracilenta* on prey species was investigated using a video mounted on an inverted microscope at a magnification of 630–1,000×.

Table 2. Design for feeding experiments

Expt No.	Experimental type	Initial predator concentration (cells mL ⁻¹)	Initial prey concentration (cells mL ⁻¹)
1	<i>Shimiella gracilenta</i>	Approximately 5,000	See Table 6
2	<i>S. gracilenta</i> with <i>Teleaulax amphioxiae</i> cells	16, 70, 393, 565, 1,142, 2,948, 5,095, 9,980	169, 888, 4,612, 7,198, 14,522, 29,198, 52,086, 103,559
	<i>S. gracilenta</i> with <i>T. amphioxiae</i> filtrate	18, 82, 411, 662, 1,336, 3,396, 5,663, 11,638	0 (filtrates corresponding to 169, 888, 4,612, 7,198, 14,522, 29,198, 52,086, 103,559)
3	<i>S. gracilenta</i> with f/2 medium	4,622	0
	<i>S. gracilenta</i> without any addition	4,849	0

Effects of prey concentration on growth and ingestion rates

Experiment 2 was conducted to determine the specific growth and ingestion rates of *S. gracilenta* SGJH1904 as a function of prey concentration (Table 2). Dense cultures of *S. gracilenta* in a 250-mL flask were transferred to 1,000-mL PC bottles with freshly filtered seawater and *T. amphioxoidea* prey (ca. 40,000 cells mL⁻¹). A dense culture of *T. amphioxoidea* in a 250-mL flask was transferred to a 1,000-mL PC bottle with f/2 medium. These stock cultures were incubated at 20°C under a 14 : 10 h light : dark cycle and 100 μmol photons m⁻² s⁻¹ of a light-emitting diode. We selected light intensity above which the maximum growth and ingestion rates of *S. gracilenta* (*G. gracilenum*) as a function of light intensity were observed (Jakobsen et al. 2000). *Shimiella gracilenta* cells were allowed to feed on prey cells for 4 days and then starved for 8 days. A negative growth rate of *S. gracilenta* (-0.1 d⁻¹) was obtained in this culture, indicating a lack of residual growth of *S. gracilenta* after feeding on prey. Three 1-mL aliquots were removed from the stock cultures, and the concentrations of *S. gracilenta* and *T. amphioxoidea* were determined.

Eight different initial concentrations of *S. gracilenta* and *T. amphioxoidea* were established using an autopipette to deliver predetermined volumes into 38-mL flasks (Table 2). Triplicate flasks with predator-prey mixtures, prey-only controls (i.e., *T. amphioxoidea* only), and predator-only controls (i.e., *S. gracilenta* only) were set up for the eight different cell concentrations of *S. gracilenta* and *T. amphioxoidea*. The stock culture of the predator *S. gracilenta* was filtered through a 0.2-μm syringe filter (DISMIC-25CS type, 25 mm; Advantec, Toyo Roshi Kaisha Ltd., Chiba, Japan). The same amount of cell-free filtrate was added to the prey-only controls as the predator culture volume was added to the predator-prey mixtures. The stock culture of *T. amphioxoidea* was filtered in the same manner. The same amount of cell-free filtrate was added to the predator-only controls as the prey culture volume was added to the predator-prey mixtures. This procedure ensured that the seawater conditions were similar to those of the predator-prey mixtures to determine the elevated growth rate as a result of predation alone. Five milliliters of f/2 medium were added to all the flasks that were then filled with freshly filtered seawater.

At the start of the incubation period, a 5-mL aliquot was taken from each flask to determine the actual concentrations of the predator and prey, and then fixed with 5% Lugol's solution. Next, each flask was refilled to capacity with freshly filtered seawater and placed on a shelf under the above conditions. Dilution due to refilling of filtered seawater into each flask was considered when the growth and ingestion rates were calculated. After a 2-day incubation period, a 10-mL aliquot was taken from each flask and fixed as described above.

Fixed *S. gracilenta* and *T. amphioxoidea* cells taken at the beginning of the incubation period and after 2 days of incubation were enumerated by counting all or >200 cells in 1-mL Sedgwick–Rafter chambers under a compound microscope.

The specific growth rate of *S. gracilenta* (μ , d⁻¹) was calculated using the following equation:

$$\mu = \frac{\ln\left(\frac{C_t}{C_0}\right)}{t} \quad (1)$$

, where C_0 and C_t represent the concentration of *S. gracilenta* at the beginning of incubation and after the elapsed time (t) of incubation, respectively.

The results for the growth rate of *S. gracilenta* with *T. amphioxoidea* cells were fitted to the Michaelis–Menten equation using DeltaGraph (SPSS Inc., Chicago, IL, USA):

$$\mu = \frac{\mu_{\max}(x - x')}{K_{GR} + (x - x')} \quad (2)$$

, where μ_{\max} is the maximum growth rate (d⁻¹), x is the concentration of *T. amphioxoidea* prey (ng C mL⁻¹), x' is the threshold prey concentration (i.e., prey concentration where $\mu = 0$), and K_{GR} is the prey concentration sustaining half of μ_{\max} .

The ingestion and clearance rates were calculated using the equation of Frost (1972) and the modified equation of Heinbokel (1978). Data for the ingestion rates of *S. gracilenta* (IR; ng C predator⁻¹ d⁻¹) were also fitted to the Michaelis–Menten equation:

$$IR = \frac{I_{\max}(x)}{K_{IR} + (x)} \quad (3)$$

, where I_{\max} is the maximum ingestion rate, and K_{IR} is the prey concentration sustaining half of I_{\max} . The carbon content of *T. amphioxoidea* was obtained from Jeong et al. (2005b).

Effects of filtrates of prey culture and f/2 medium on the growth rate

Experiment 3 was conducted to determine whether filtrates of stock cultures of *T. amphioxoidea* (i.e., without prey cells) or f/2 medium affected the growth rates of *S. gracilenta*.

lenta SGJH1904. The growth rates of *S. gracilenta* with *T. amphioxoidea* cells, only *T. amphioxoidea* filtrates, only f/2 medium, and without any addition were compared (Table 2). Data on the growth rates of *S. gracilenta* with *T. amphioxoidea* cells and without prey cells but filtrates (i.e., predator-only controls) were obtained from the results of experiment 2. For experiments involving the addition of f/2 medium or no additions, *S. gracilenta* cells were saturated with *T. amphioxoidea* for 14 days, followed by starvation for 26 days. At this point, the growth rate of *S. gracilenta* was negative (-0.1 d⁻¹). A single high concentration of *S. gracilenta* (5,000 cells mL⁻¹) was set up in triplicate. The growth rate of *S. gracilenta* was determined as described previously.

Statistical analysis

Pearson's correlation analysis was used to test the relationships between the abundance of *S. gracilenta* and biotic / abiotic factors. Data on the abundances of *T. amphioxoidea* and *Pyramimonas* sp. at 28 stations from 2015 to 2018 were obtained from Jang and Jeong (2020). One-way analysis of variance (ANOVA) with a post-hoc Tukey's honestly significant difference test was used to compare the growth rates of *S. gracilenta* SGJH1904 with *T. amphioxoidea* cells, only *T. amphioxoidea* filtrates, f/2 medium, and without any addition. The normality and homogeneity of the data were tested prior to the one-way ANOVA analysis. Statistical significance was set at $p < 0.05$. All statistical analyses were performed using SPSS ver. 25.0 (IBM-SPSS Inc., Armonk, NY, USA).

RESULTS

Specificity test and standard curve construction

The species specificity of the primer and probe set developed in this study was tested using *S. gracilenta* SGHJ1904 and the other 25 species (Supplementary Table S3). *Shimiella gracilenta* was positively detected, whereas the remaining species were negatively detected.

The standard curve indicated high linearity between log cell number and cycle threshold (Ct) with $r^2 = 0.996$ (Supplementary Fig. S1). The slope for Ct as a function of log cell abundance was -3.18, which corresponds to an efficiency of 106%.

Spatial distributions in Korean waters

Using the primer and probe set developed in this study, the abundance of *S. gracilenta* in water samples from 28 stations from April 2015 to October 2018 was quantified (Table 3). Cells of *S. gracilenta* were detected at all the 28 stations from 2015 to 2018, indicating its wide spatial distribution. However, its cell abundance in Korean coastal waters in 2015 to 2018 was very low (Table 3); the highest abundance of *S. gracilenta* (2.96 cells mL⁻¹) was found in Seogwipo (Jeju Island), and the second highest abundance (2.25 cells mL⁻¹) was in the waters off Ansan.

Temporal distributions in Korean waters

Cells of *S. gracilenta* were detected during all four seasons: 18 stations in spring and summer, 16 stations in autumn, and 13 stations in winter (Fig. 2). The highest and second highest abundances of *S. gracilenta* (2.96 and 2.25 cells mL⁻¹, respectively) were found in the summer of 2016 and 2017, respectively (Table 3, Fig. 2B). In spring, autumn, and winter seasons in 2015 to 2018, the highest abundances of *S. gracilenta* were <1 cell mL⁻¹ (Fig. 2A, C & D): 0.71 cells mL⁻¹ in spring, 0.61 cells mL⁻¹ in autumn, and 0.63 cells mL⁻¹ in winter (Table 3).

Hydrographic and biological properties

Abiotic environmental factors, such as water temperature, salinity, and DO, varied greatly between 2015 and 2018 (Table 4). Cells of *S. gracilenta* were detected in Korean coastal waters when water temperature, salinity, and DO ranged 1.7–26.4°C, 9.9–35.6, and 0.7–14.2 mg L⁻¹, respectively (Table 4). Furthermore, when *S. gracilenta* was detected, the concentrations of NO₃, PO₄, and SiO₂ were in between ND–107.1, ND–6.3, and ND–448.4 μM, respectively. The highest abundance of *S. gracilenta* (2.96 cells mL⁻¹) was detected when the water temperature and salinity were 20.4°C and 17.5, respectively (Fig. 3A); moreover, this abundance value was observed when NO₃ and PO₄ concentrations were 43.0 and 0.90 μM, respectively (Fig. 3B). However, *S. gracilenta* abundance was significantly correlated with water temperature and salinity, but not with DO, NO₃, PO₄, and SiO₂ (Table 4).

Biotic factors such as Chl-a and the abundance of the prey species *T. amphioxoidea* or *Pyramimonas* sp. from 2015 to 2018 also varied considerably (Table 4). Cells of *S. gracilenta* were detected when Chl-a ranged from 0.2 to 59.1 μg L⁻¹. Moreover, *S. gracilenta* was also detected when the abundances of *T. amphioxoidea* and *Pyramimonas* sp.

Table 3. Abundances (cells mL⁻¹) of *Shimiella gracilenta* at each station from April 2015 to October 2018, quantified using quantitative real-time polymerase chain reactions

St.	Name	2015		2016		2017		2018									
		Apr	Jul	Oct	Jan	Mar	Jun-Jul	Sep-Oct	Dec	Mar	Jul	Oct	Jan-Feb	Mar	Jul	Oct	Max
SC	Sokcho	-	-	-	-	-	-	0.01	NA	-	-	-	-	-	-	-	0.01
JMJ	Jumunjin	0.05	-	-	-	-	0.01	-	-	-	-	-	-	-	-	0.30	
DH	Donghae	-	0.25	0.03	-	-	0.01	-	0.06	-	0.08	-	-	-	-	-	0.30
UJ	Ujin	-	-	-	0.03	-	-	-	-	-	0.10	-	-	-	-	-	0.01
PH	Pohang	-	-	-	-	-	0.51	-	-	-	-	0.19	-	-	-	0.16	0.16
US	Ulsan	-	-	-	-	0.55	0.05	-	-	-	0.25	-	-	-	-	-	0.51
BS	Busan	-	-	-	-	-	0.50	-	-	-	0.19	-	-	-	-	-	0.55
DDP	Dadaepo	-	-	-	-	0.05	-	-	-	0.18	0.30	-	-	-	-	-	0.50
JH	Jinhae	NA	-	-	-	-	2.10	-	0.40	0.60	0.14	-	-	-	-	-	0.30
MS	Masan	-	-	-	0.01	-	-	0.20	0.63	-	-	-	-	-	-	-	2.10
TY	Tongyeong	-	-	-	-	0.10	-	-	-	0.66	-	-	-	-	-	-	0.63
YS	Yeosu	NA	-	-	-	-	-	-	-	-	0.01	-	-	-	-	-	0.66
KY	Kwangyang	-	-	-	-	-	-	-	-	-	-	-	-	-	-	-	0.01
GH	Goheung	NA	-	-	-	-	-	-	0.30	-	-	-	-	-	-	-	0.30
IAH	Jangheung	-	0.28	-	-	0.04	-	-	-	-	-	-	-	-	-	-	0.28
AS	Ansan	-	-	0.06	-	-	0.13	-	-	-	2.25	-	-	-	-	-	0.25
DAJ	Dangjin	0.25	-	-	-	-	-	-	0.06	0.09	-	-	-	-	-	0.01	0.25
MGP	Mageompo	-	0.09	0.04	0.10	0.04	0.36	0.61	-	-	0.33	-	-	-	-	-	0.61
TA	Taeon	0.40	-	-	0.19	NA	0.08	-	0.10	NA	NA	NA	NA	NA	NA	NA	0.40
SCN	Seocheon	-	-	-	-	0.04	-	-	-	-	-	-	-	-	-	-	0.04
KS	Kunsan	-	0.31	-	-	0.71	1.54	0.11	-	0.03	0.11	-	-	-	-	-	1.54
BA	Buan	-	0.60	-	0.16	0.53	0.15	-	-	0.11	0.05	-	-	-	-	-	0.60
MP	Mokpo	-	-	-	0.08	-	0.19	-	-	0.08	-	-	-	-	-	-	0.54
AW	Aewol	-	-	-	-	-	0.06	-	-	NA	NA	NA	NA	NA	NA	NA	0.06
SGP	Segwipo	-	-	-	0.03	2.96	-	-	0.06	-	-	-	-	-	-	-	2.96
WM	Wimi	0.06	-	-	0.03	-	-	-	-	-	-	-	-	-	-	-	0.34
SS	Seongsan	-	-	-	-	NA	NA	0.19	0.10	-	-	-	-	-	-	-	0.19
GN	Gimnyeong	NA	NA	NA	NA	NA	NA	NA	NA	0.15	-	-	-	-	-	-	0.15

St., station; Max., maximum abundance of *S. gracilenta* at each station (cells mL⁻³); -, not detected; NA, samples were not available. March and April, spring; June and July, summer; September and October, autumn; December, January, and February, winter.

Table 4. Ranges of the abiotic and biotic factors in Korean coastal waters from April 2015 to October 2018 during the study period and when *Shimiella gracilenta* was detected

Type	Abiotic factor						Biotic factor		
	T (°C)	Salinity (mg L ⁻¹)	DO (mg L ⁻¹)	NO ₃ (µM)	PO ₄ (µM)	SiO ₂ (µM)	Chl-a (µg L ⁻¹)	Teleaulax amphioxidea (cells mL ⁻¹)	Pyramimonas sp. (cells mL ⁻¹)
The study period	0.2–28.0	ND–35.6	0.2–14.8	ND–149.0	ND–6.3	ND–453.4	0.1–127.0	0–666.5	0–917.6
When <i>S. gracilenta</i> was detected	1.7–26.4	9.9–35.6	0.7–14.2	ND–107.1	ND–6.3	ND–448.4	0.2–59.1	0–666.5	0–917.6
Pearson's correlation coefficients (<i>r</i>) ^a	0.207*	-0.409**	-0.060	0.167	0.037	0.204	0.044	0.019	0.034

Data of T and salinity during the study period were from Lee et al. (2019b) and the rest data were from Kang et al. (2019) and Jang and Jeong (2020). T, water temperature; DO, dissolved oxygen; NO₃, nitrite and nitrate concentration (NO₂ + NO₃); PO₄, phosphate concentration; SiO₂, silicate concentration; Chl-a, chlorophyll-a concentration; ND, not detected.

^aThe relationships between *S. gracilenta* abundance (cells mL⁻¹) and environmental factors when *S. gracilenta* was detected.

*p < 0.05, **p < 0.01.

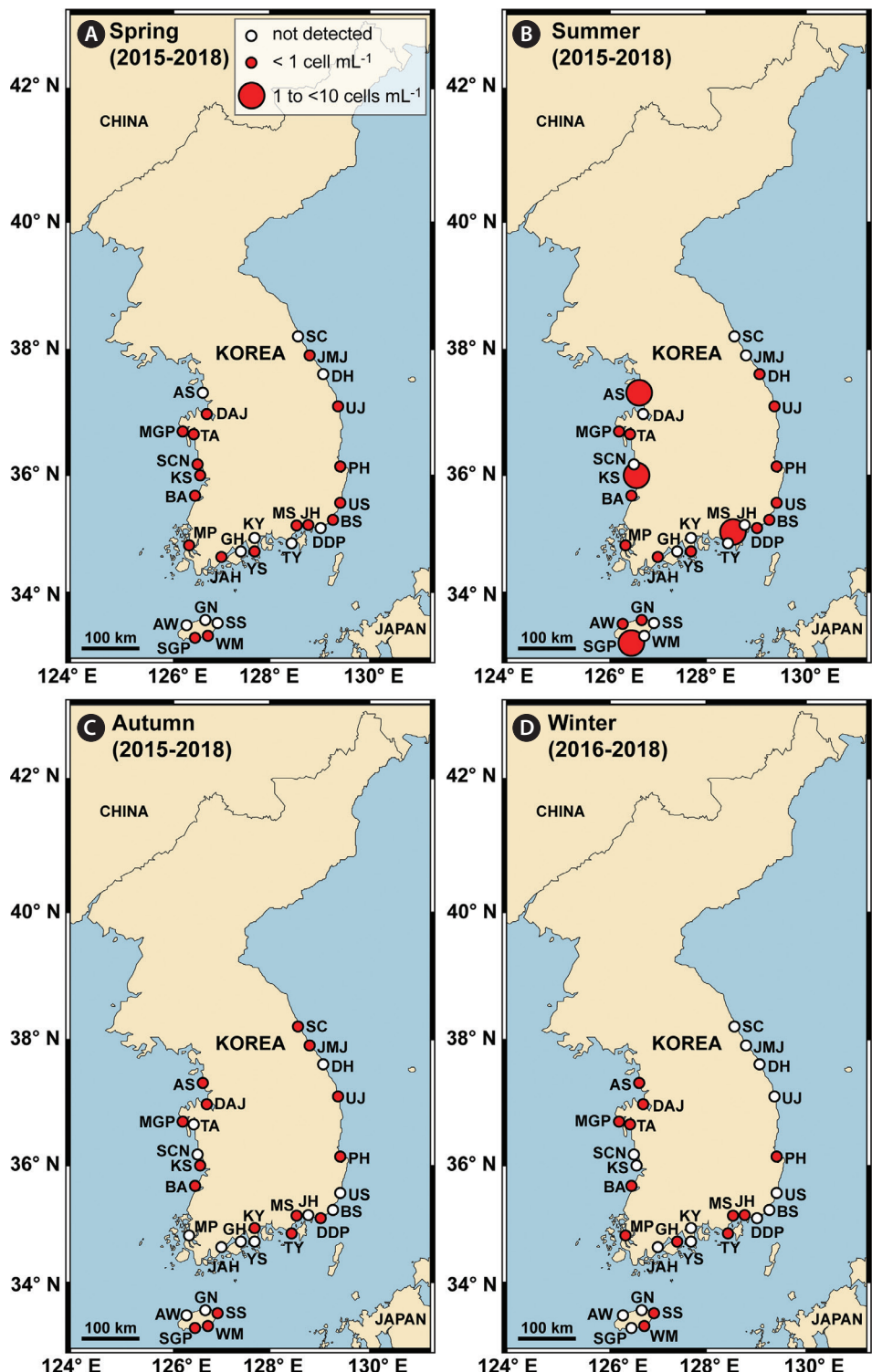


Fig. 2. Map of the sampling stations indicating the presence or absence of *Shimiella gracilenta* during April 2015–October 2018. (A) Spring (March or April). (B) Summer (June or July). (C) Autumn (September or October). (D) Winter (December, January, or February). The red closed circles indicate the stations where *S. gracilenta* cells were detected, whereas black open circles indicate the stations where *S. gracilenta* cells were not detected. The size of the red closed circles represents the abundance of *S. gracilenta* cells. SC, Sokcho; JMJ, Jumunjin; DH, Donghae; UJ, Uljin; PH, Pohang; US, Ulsan; BS, Busan; DDP, Dadaepo; MS, Masan; JH, Jinhae; TY, Tongyoung; YS, Yeosu; KY, Kwangyang; GH, Goheung; JAH, Jangheung; AS, Ansan; DAJ, Dangjin; MGP, Mageompo; TA, Taean; SCN, Seocheon; KS, Kunsan; BA, Buan; MP, Mokpo; AW, Aewol; SGP, Seogwipo; WM, Wimi; SS, Seongsan; GN, Gimnyeong.

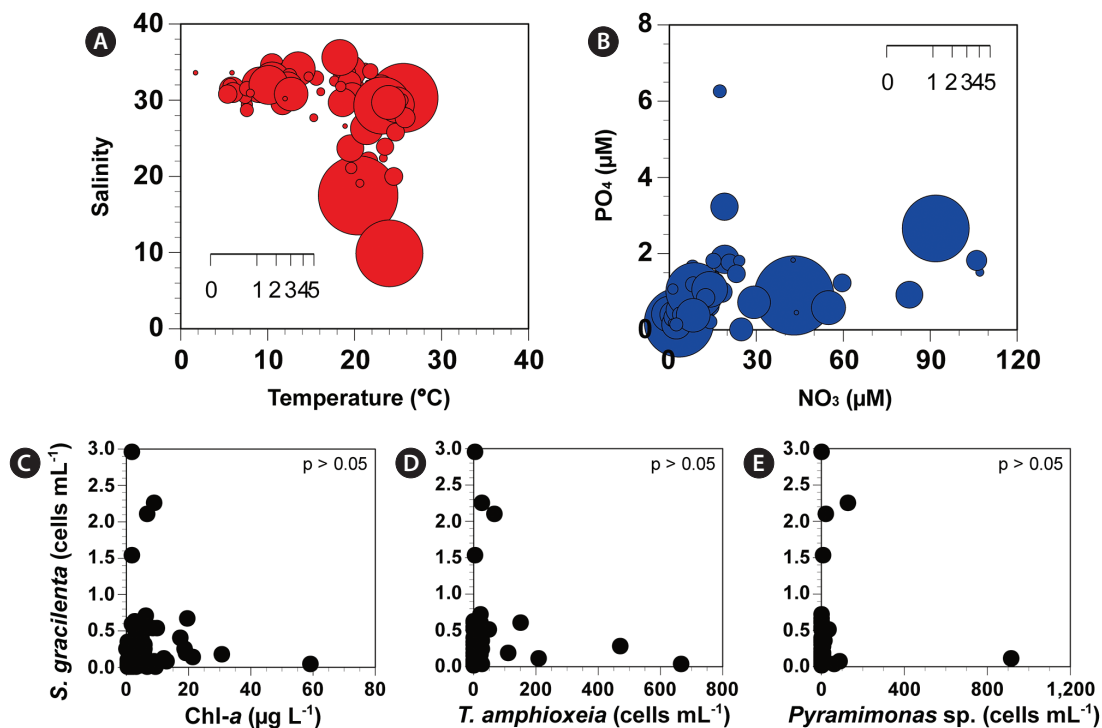


Fig. 3. Abundances (cells mL^{-1}) of *Shimiella gracilenta* as a function of each abiotic / biotic factors at stations where *S. gracilenta* cells were detected from April 2015 to October 2018. Abundance as a function of water temperature and salinity (A), NO_3 and PO_4 (B), Chl- a (C), the abundance of prey *Teleaulax amphioxiae* (D), and the abundance of prey *Pyramimonas* sp. (E). Circle diameters in (A) and (B) scaled to the abundance of *S. gracilenta*.

were 0–666.5 and 0–917.6 cells mL^{-1} , respectively. However, the abundance of *S. gracilenta* was not significantly correlated with Chl- a or abundance of *T. amphioxiae* or *Pyramimonas* sp. (Table 4, Fig. 3C–E).

Confirmation on the presence of *Shimiella gracilenta*

The sequences of ITS rDNA of the five *S. gracilenta* strains (SGMGP210406, SGDA210406, SGJG210428, SGHJ210428, and SGDA210429) were 100% identical to that of *S. gracilenta* SGJH1904 (Table 5).

When the qPCR method was used, the abundance of *S.*

gracilenta in the water samples at stations where the cells of the five strains were isolated ranged from 0.31 to 2.94 cells mL^{-1} (Table 5). The water temperature and salinity when these five strains were isolated ranged 9.6–14.9°C and 29.2–31.3, respectively (Table 5).

Prey type

Among the microalgal and ciliate species that were provided as prey, *S. gracilenta* SGJH1904 was observed to feed on the prymnesiophytes *Chrysochromulina* sp. and *P. antarctica*, the cryptophytes *T. amphioxiae*, *Storeatula major*, *Rhodomonas salina*, the prasinophyte *Pyramimonas* sp.,

Table 5. Information on *Shimiella gracilenta* strains collected in April 2021, sequence identity, and their abundance (cells mL^{-1}) quantified using qPCR

Strain name	Collection area	Collection date	T (°C)	Salinity	Sequence identity (%)	Abundance
SGMGP210406	Mageompo, Korea	Apr 6, 2021	9.6	31.3	100	2.94
SGDA210406	Taean, Korea	Apr 6, 2021	11.0	31.3	100	0.31
SGJG210428	Dangjin, Korea	Apr 28, 2021	12.2	30.1	100	0.81
SGHJ210428	Dangjin, Korea	Apr 28, 2021	13.9	29.2	100	1.03
SGDA210429	Taean, Korea	Apr 29, 2021	14.9	30.8	100	2.66

Sequence identity of the five strains against that of *S. gracilenta* SGJH1904 (GenBank accession No. MN965778) in the internal transcribed spacer ribosomal DNA region was compared using megaBLAST in the NCBI BLAST. qPCR, quantitative real-time polymerase chain reaction; T, water temperature.

and the dictyochophyte *Apedinella* sp. (Table 6). The ESD of these prey species were $\leq 8.8 \mu\text{m}$ (Table 6). Under a light microscope, yellowish, greenish, or reddish prey materials were observed inside the protoplasm of *S. gracilenta* cells (Fig. 4). However, *S. gracilenta* cells did not feed on the prymnesiophyte *Isochrysis galbana*, the chlorophyte *Dunaliella salina*, the dictyochophyte *Pseudopedinella elastica*, the raphidophyte *Heterosigma akashiwo*, the diatom *Skeletonema costatum*, all the dinoflagellates tested in this study, and the ciliate *M. rubrum* (Table 6). Among these microalgal and ciliate species, although *S. gracilenta* was found to attack *I. galbana* and *S. costatum*, it failed to ingest these two species.

Feeding mechanism

Shimiella gracilenta SGJH1904 fed on a *R. salina* cell using a peduncle (Fig. 5). The materials (yellow) were observed to be transported from the prey to the predator through a thin peduncle.

Effects of prey concentration on the growth rate

With increasing mean prey concentrations, the specific growth rate of *S. gracilenta* SGJH1904 on *T. amphioxiae* rapidly increased at mean prey concentrations of $\leq 199 \text{ ng C mL}^{-1}$ ($11,697 \text{ cells mL}^{-1}$). However, it became saturated

Table 6. Taxa, size, and concentration of algal prey species offered to *Shimiella gracilenta* SGJH1904, and feeding occurrence

Organisms	Strain name	ESD (μm)	Initial cell density (cells mL^{-1})	Attack	Feeding
Prymnesiophyte					
<i>Chrysocromulina</i> sp.	CSYS1905	3.1	700,000	○	○
<i>Phaeocystis antarctica</i>	RCC4023	3.1	500,000	○	○
<i>Isochrysis galbana</i>	IG	4.8	300,000	○	×
Cryptophyte					
<i>Teleaulax amphioxiae</i>	TSGS0202	5.6	150,000	○	○
<i>Storeatula major</i>	SSSH1103	6.0	100,000	○	○
<i>Rhodomonas salina</i>	RS	8.8	50,000	○	○
Prasinophyte					
<i>Pyramimonas</i> sp.	PSSH1204	5.6	150,000	○	○
Chlorophyte					
<i>Dunaliella salina</i>	DSJH1710	10.3	30,000	×	×
Dictyochophyte					
<i>Apedinella</i> sp.	ASGY1807	7.0	50,000	○	○
<i>Pseudopedinella elastica</i>	PEJH1904	7.9	50,000	×	×
Raphidophyte					
<i>Heterosigma akashiwo</i>	HAKS9905	11.5	30,000	×	×
Diatom					
<i>Skeletonema costatum</i>	SCYS1801	5.9	150,000	○	×
Dinoflagellate					
<i>Heterocapsa rotundata</i>	HRSH1201	5.8	50,000	×	×
<i>Amphidinium carterae</i>	SIO PY-1	9.7	30,000	×	×
<i>Effrenium voratum</i>	SvFL 1	11.1	30,000	×	×
<i>Prorocentrum cordatum</i>	PMKS9906	12.1	15,000	×	×
<i>Karlodinium veneficum</i>	KVJH1607	12.5	30,000	×	×
<i>Heterocapsa steinii</i>	HTMS0806	15.0	15,000	×	×
<i>Alexandrium minutum</i>	CCMP1888	20.4	10,000	×	×
<i>Karenia mikimotoi</i>	NIES-2411	21.3	3,000	×	×
<i>Scrippsiella acuminata</i>	STGP9909	22.8	10,000	×	×
<i>Margalefidinium polykrikoides</i>	CPWD1509	25.9	3,000	×	×
<i>Prorocentrum micans</i>	PMSH0910	26.6	3,000	×	×
<i>Akashiwo sanguinea</i>	ASUSA	30.8	1,000	×	×
<i>Tripos furca</i>	TFDD1808	28.9	2,000	×	×
<i>Alexandrium fraterculus</i>	AFYS1309	32.3	2,000	×	×
<i>Lingulodinium polyedra</i>	CCMP1931	38.2	1,500	×	×
Ciliate					
<i>Mesodinium rubrum</i>	MR-MAL01	22.0	2,000	×	×

ESD, equivalent spherical diameter; ○, attacked or fed by *S. gracilenta*; ×, not attacked or fed by *S. gracilenta*.

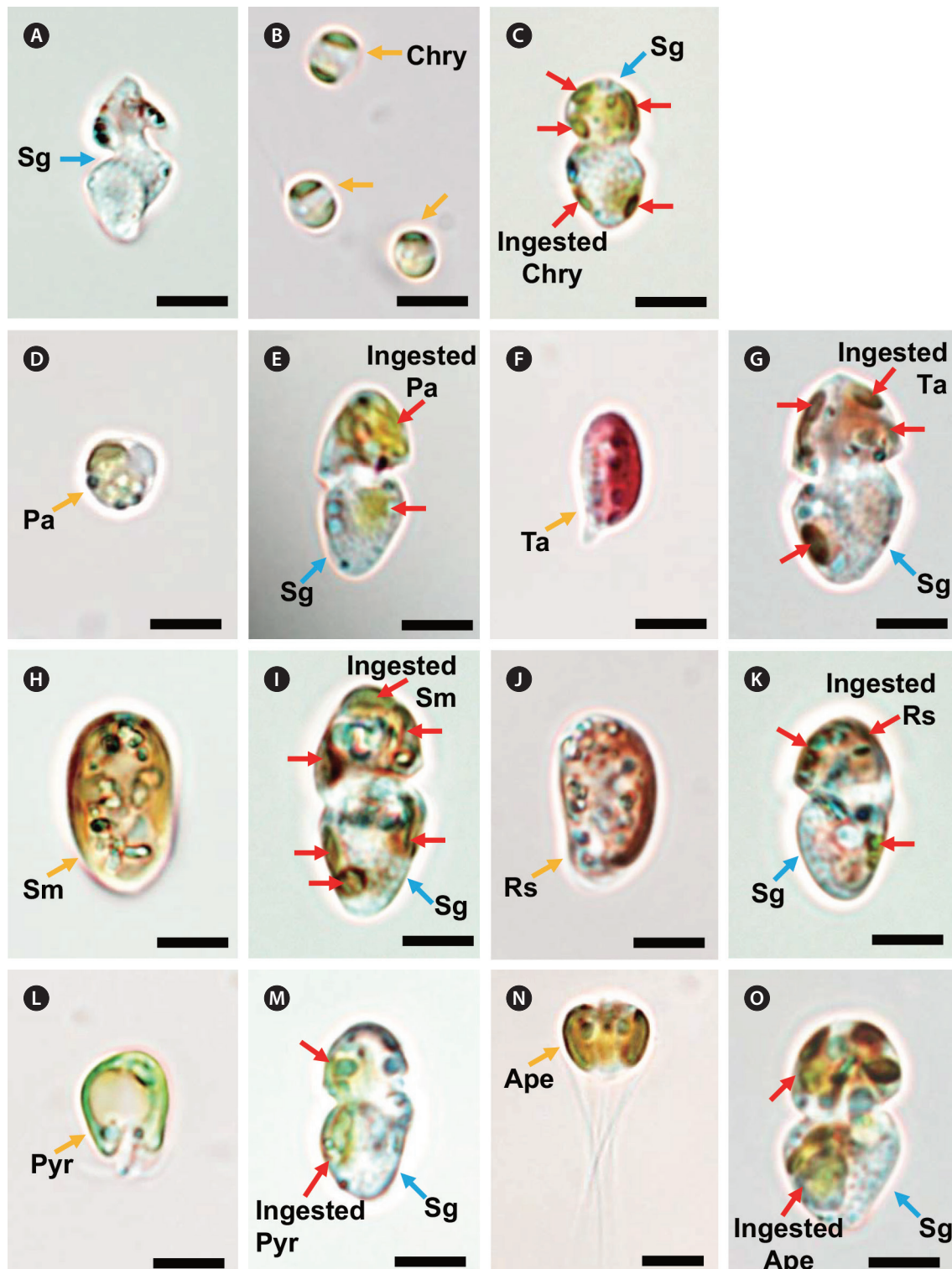


Fig. 4. Feeding by the kleptoplastidic dinoflagellate *Shimiella gracilenta* SGJH1904 (Sg) on algal prey species. (A) A starved Sg cell. (B) Intact *Chrysochromulina* sp. (Chry) cells. (C) Sg with ingested Chry cells. (D) An intact *Phaeocystis antarctica* (Pa) cell. (E) Sg with ingested Pa cells. (F) An intact *Teleaulax amphioxidea* (Ta) cell. (G) Sg with ingested Ta cells. (H) An intact *Storeatula major* (Sm) cell. (I) Sg with ingested Sm cells. (J) An intact *Rhodomonas salina* (Rs) cell. (K) Sg with ingested Rs cells. (L) An intact *Pyramimonas* sp. (Pyr) cell. (M) Sg with ingested Pyr cells. (N) An intact *Apedinella* sp. (Ape) cell. (O) Sg with ingested Ape cells. Scale bars represent: A–O, 5 μ m.

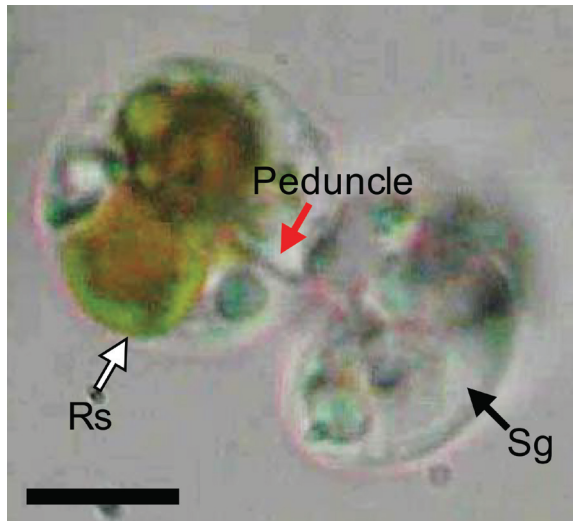


Fig. 5. Feeding by the kleptoplastidic dinoflagellate *Shimiella gracilenta* SGJH1904 (Sg) on the cryptophyte *Rhodomonas salina* (Rs) cell. The red arrow indicates the peduncle of Sg. Scale bar represents: 5 μm .

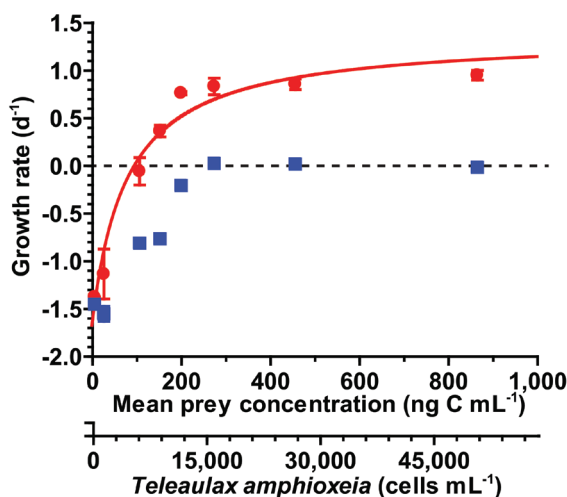


Fig. 6. Specific growth rates of *Shimiella gracilenta* SGJH1904 feeding on *Teleaulax amphioxeia* cells as a function of mean prey concentration (x , ng C mL^{-1} ; red circles) or its filtrate of corresponding mean prey concentration (blue squares) (see Table 2). Symbols represent the treatment mean \pm standard error. The curves were fitted to a Michaelis-Menten equation (Eq. 2). Growth rate (d^{-1} ; red line) = $1.36 \left[(x - 95.5) / \{173 + (x - 95.5)\} \right]$, $r^2 = 0.957$.

at higher mean prey concentrations (Fig. 6). When these data were fitted to equation (2), the μ_{\max} and K_{GR} of *S. gracilenta* feeding on *T. amphioxeia* were 1.36 d^{-1} and 173 ng C mL^{-1} ($10,176 \text{ cells mL}^{-1}$), respectively. The threshold prey concentration for the growth of *S. gracilenta* was $95.5 \text{ ng C mL}^{-1}$ ($5,618 \text{ cells mL}^{-1}$). The highest specific growth rate of *S. gracilenta* with *T. amphioxeia* filtrate (without *T. amphioxeia* prey cells) was 0.03 d^{-1} (Fig. 6).

Effects of filtrates of prey culture and f/2 medium on the growth rate

At a single high *S. gracilenta* concentration ($5,000 \text{ cells mL}^{-1}$), the specific growth rates of *S. gracilenta* SGJH1904 with *T. amphioxeia* cells, only *T. amphioxeia* filtrates, f/2 medium, and without any addition were significantly different (one-way ANOVA, $F_{3,8} = 242.3$, $p < 0.001$) (Fig. 7). The growth rate of *S. gracilenta* with *T. amphioxeia* filtrate (0.02 d^{-1}) was significantly higher than that with f/2 medium (-0.15 d^{-1}) or without any additions (-0.24 d^{-1}).

Effects of prey concentration on the ingestion rate

With increasing mean prey concentrations, the ingestion rate of *S. gracilenta* SGJH1904 on *T. amphioxeia* increased rapidly at mean prey concentrations of $\leq 199 \text{ ng C mL}^{-1}$ ($11,697 \text{ cells mL}^{-1}$), but became saturated at higher mean prey concentrations (Fig. 8). When these data were fitted to equation (3), the I_{\max} and K_{IR} of *S. gracilenta* feeding on *T. amphioxeia* were $0.04 \text{ ng C predator}^{-1} \text{ d}^{-1}$ ($2.35 \text{ cells predator}^{-1} \text{ d}^{-1}$) and $10.5 \text{ ng C mL}^{-1}$ ($618 \text{ cells mL}^{-1}$), respectively.

DISCUSSION

The present study demonstrates that *S. gracilenta* has a wide spatial distribution in Korean coastal waters from $33^{\circ}14' \text{ N}$ to $38^{\circ}10' \text{ N}$. Prior to the present study, *S. gracilenta* was reported in the waters from 29° N to 80° N ; Kuwait coastal waters (29° N) (Al-Mutairi et al. 2020), U. S. coastal waters (34° N) (Campbell 1973), Korean coastal waters (35° N) (Ok et al. 2021a), Scandinavian waters ($51\text{--}55^{\circ} \text{ N}$) (Skovgaard 1998, Martin and Gypens 2021), and the Arctic Ocean ($69\text{--}80^{\circ} \text{ N}$) (de Sousa 2020, Back et al. 2021). These regions are all located in the northern hemisphere, and *S. gracilenta* cells have not been reported to be present in the Southern Hemisphere. Hence, additional data on the distribution and abundance of *S. gracilenta* on a global geographic scale are needed.

In the present study, *S. gracilenta* was found during all four seasons in the period from 2015 to 2018 and at $1.7\text{--}26.4^{\circ}\text{C}$, indicating that *S. gracilenta* has a wide temporal distribution. However, the highest abundance of *S. gracilenta* was observed in summer when the water temperature was 20.4°C in the study area. Furthermore, the abundance of *S. gracilenta* was positively correlated with water temperature. In addition, Campbell (1973), who

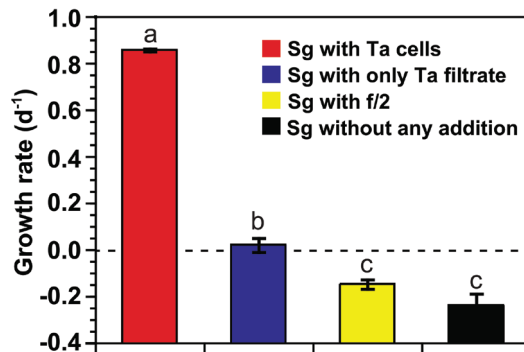


Fig. 7. Comparisons of specific growth rates of *Shimiella gracilenta* SGJH1904 (Sg) under different nutritional conditions (with *Teleaulax amphioxeia* [Ta] cells, only Ta filtrates, and f/2 medium, and without any addition) at a single high Sg concentration. The lowercase alphabetical letters above each bar indicate significantly different groups divided by a post-hoc Tukey's honestly significant difference test.

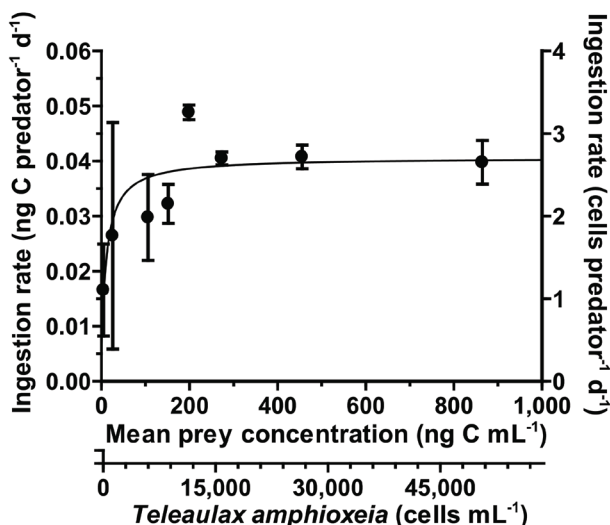


Fig. 8. Ingestion rates of *Shimiella gracilenta* SGJH1904 feeding on *Teleaulax amphioxeia* as a function of mean prey concentration (x, ng C mL⁻¹). Symbols represent the treatment mean \pm standard error. The curve was fitted to a Michaelis–Menten equation (Eq. 3). Ingestion rate (ng C predator⁻¹ d⁻¹) = 0.04 [x / (10.5 + x)], $r^2 = 0.267$.

had first described *S. gracilenta* (reported as *G. gracilellum*), reported that the highest abundance in Gales Creek was observed in summer (18 cells mL⁻¹). This evidence suggests that the abundance of *S. gracilenta* is seasonal.

The abundance of *S. gracilenta* was negatively correlated with salinity. The salinity range when *S. gracilenta* cells were detected was very wide (9.9–35.6). Campbell (1973) also reported that this species was present in a similar salinity range of 9–30. Thus, *S. gracilenta* may survive in estuaries, where salinity fluctuates due to freshwater or effluent inputs. In Kuwait Bay, *S. gracilenta* was observed

under a microscope at a salinity of approximately 44 (Al-Mutairi et al. 2020). Thus, *S. gracilenta* can survive under high-salinity conditions. Therefore, the reported salinity range of *S. gracilenta* cells was from 9 to 44, indicating that it is a euryhaline species. Overall, these euryhaline and eurythermal characteristics of *S. gracilenta* may be partially responsible for its wide spatial and temporal distributions in Korean waters.

The growth rate of *S. gracilenta* SGJH1904 was largely affected by *T. amphioxeia* prey concentration; thus, prey availability may strongly affect its abundance. *Shimiella gracilenta* (*G. gracilellum*) has been known to feed on cryptophytes *Chroomonas* sp., *Plagioselmis prolonga*, *Rhodomonas marina*, *R. salina*, and *T. amphioxeia* (Jakobsen et al. 2000). However, the present study clearly showed that *S. gracilenta* was able to feed on prymnesiophytes, a prasinophyte, a dictyochophyte, and another cryptophyte *S. major*. Moreover, *S. gracilenta* can reportedly utilize kleptoplastidy to survive for approximately one month in the absence of prey (Ok et al. 2021a). Thus, its ability to feed on diverse prey and conduct kleptoplastidy may also contribute to the wide spatial and temporal distributions of *S. gracilenta* in Korean waters.

In the present study, the highest abundance of *S. gracilenta* was only 2.96 cells mL⁻¹, although cells were detected in all the 28 stations. The threshold *T. amphioxeia* prey concentration for *S. gracilenta* (i.e., no growth) in the present study was 5,618 cells mL⁻¹ (95.5 ng C mL⁻¹). However, the highest abundance of *T. amphioxeia* during the study period was 667 cells mL⁻¹ (11.3 ng C mL⁻¹). Using the equation in Fig. 6 and the abundance of *T. amphioxeia* during the study period from 2015 to 2018, the calculated specific growth rates of *S. gracilenta* on *T. amphioxeia* were negative (-1.7 to -1.3 d⁻¹). Therefore, the abundance of *T. amphioxeia* in Korean waters during the study period was likely insufficient to support the positive growth of *S. gracilenta*. Furthermore, in the present study, the abundance of *S. gracilenta* was not significantly correlated with the abundance of *T. amphioxeia* or *Pyramimonas* sp. The low abundance of *T. amphioxeia* or *Pyramimonas* sp. may be partially responsible for this insignificant correlation. However, the maximum growth rates of *S. gracilenta* on suitable prey species were 1.36–1.51 d⁻¹, which are among the highest maximum growth rates of dinoflagellates feeding on *T. amphioxeia* (Table 7). Thus, there is a possibility that the abundance of *S. gracilenta* rapidly increases if the abundance of *T. amphioxeia* is higher than 5,618 cells mL⁻¹ in natural environments. The abundance of cryptophytes, including the genus *Teleaulax*, in natural seawater, has been reported

as 392,440 cells mL^{-1} (6,671 ng C mL^{-1}) in Masan Bay, Korea, 15,720 cells mL^{-1} (267 ng C mL^{-1}) in Chesapeake Bay, USA, and 2,173 cells mL^{-1} (37 ng C mL^{-1}) in Blanes Bay, Spain (Jeong et al. 2013, Johnson et al. 2013, Unrein et al. 2014). Assuming that all cryptophytes are *T. amphioxiae* in natural seawaters, the specific growth rates of *S. gracilenta* were calculated to be 1.33 d^{-1} in Masan Bay, 0.68 d^{-1} in Chesapeake Bay, and -0.70 d^{-1} in Blanes Bay. Therefore, *S. gracilenta* is expected to be highly abundant in Masan Bay, moderately abundant in Chesapeake Bay, and rare in Blanes Bay under these prey concentrations.

When *S. gracilenta* was detected during 2015–2018, the highest Chl- a was 59 ng mL^{-1} , which was calculated to be 2,360 ng C mL^{-1} , assuming a carbon to chlorophyll ratio of 40 (Cloern et al. 1983, Peterson and Festa 1984). This carbon value is much higher than the threshold *T. amphioxiae* prey concentration for *S. gracilenta*. Based on the results of high Chl- a but low abundance of *S. gracilenta* during the study period, it is suggested that phytoplankton species that are not fed on by *S. gracilenta* may have contributed to the high Chl- a .

Identifying *S. gracilenta* in field samples under a light microscope is difficult because cells of *S. gracilenta* are very small ($9.3 \mu\text{m}$ in ESD) (Park et al. 2021) and fragile. Since the abundance of *S. gracilenta* during 2015–2018 was generally low, this study confirmed the detection of *S. gracilenta* by qPCR using a suitable prey enrichment

and incubation method. The present study successfully confirmed that *S. gracilenta* cells were present even when $<1 \text{ cell mL}^{-1}$ of *S. gracilenta* was detected by qPCR. In conclusion, the qPCR method used in the present study is a suitable method for quantifying *S. gracilenta* abundance in natural seawaters, as well as a suitable prey enrichment and incubation method for confirming the presence of low abundance of *S. gracilenta*.

The I_{\max} of *S. gracilenta* on *T. amphioxiae* in the present study and the literature ($0.04\text{--}0.08 \text{ ng C predator}^{-1} \text{ d}^{-1}$) is comparable to that of the mixotrophic dinoflagellates *Prorocentrum donghaiense*, *Prorocentrum micans*, *Heterocapsa steinii*, and *Gymnodinium aureolum* ($0.03\text{--}0.06 \text{ ng C predator}^{-1} \text{ d}^{-1}$), but lower than that of many mixotrophic, kleptoplastidic, and heterotrophic dinoflagellates on the same prey species (Table 7). Furthermore, the peduncle-feeding *S. gracilenta* has an I_{\max} comparable to that of *G. aureolum* but lower than that of other peduncle-feeding dinoflagellates ($0.18\text{--}1.10 \text{ ng C predator}^{-1} \text{ d}^{-1}$). Although the I_{\max} of *S. gracilenta* on *T. amphioxiae* was relatively low, the μ_{\max} of *S. gracilenta* on *T. amphioxiae* was greater than that of the other dinoflagellates on the same prey species. The ratio of the newly produced carbon by *S. gracilenta* SGJH1904 to ingested prey carbon, calculated as described by Skovgaard (1998), was >1.0 . Thus, *S. gracilenta* SGJH1904 may conduct kleptoplastidy during satiation with prey cells as well as starvation.

Table 7. Comparison of the maximum growth and ingestion rates of dinoflagellate predators feeding on the cryptophyte *Teleaulax amphioxiae*

Predator	Type	Feeding mechanism	ESD	μ_{\max}	I_{\max}	Reference
<i>Shimiella gracilenta</i>	KPD	Peduncle	9.3	1.36	0.04	Park et al. (2021), This study
<i>Shimiella gracilenta</i> ^a	KPD	Peduncle	9.8 ^b	1.51	0.08 ^c	Skovgaard (1998), Jakobsen et al. (2000)
<i>YihIELLA yeosuensis</i> ^a	MTD	Engulfment	7.8	1.29	0.38	Jang et al. (2017)
<i>Pfiesteria piscicida</i>	KPD	Peduncle	8.7 ^d	1.15	1.10	Burkholder et al. (2001), Jeong et al. (2006)
<i>Gyrodiniellum shiwhaense</i>	HTD	Peduncle	12.7	1.05	0.35	Jeong et al. (2011)
<i>Paragymnodinium shiwhaense</i> ^a	MTD	Peduncle	12.4	0.64	0.18	Yoo et al. (2010)
<i>Prorocentrum donghaiense</i>	MTD	Engulfment	13.3	0.51	0.03	Jeong et al. (2005a)
<i>Margalefidinium polykrikoides</i>	MTD	Engulfment	23.1	0.32	0.16	Jeong et al. (2004)
<i>Heterocapsa steinii</i>	MTD	Engulfment	15.0	0.28	0.04	Jeong et al. (2005a)
<i>Gonyaulax polygramma</i>	MTD	Engulfment	32.5	0.28	0.18	Jeong et al. (2005b)
<i>Luciella masanensis</i>	HTD	Peduncle	13.5	0.24	0.44	Jeong et al. (2007)
<i>Prorocentrum micans</i>	MTD	Engulfment	26.6	0.20	0.04	Jeong et al. (2005a)
<i>Gymnodinium aureolum</i> ^a	MTD	Peduncle	19.4	0.17	0.06	Jeong et al. (2010a)
<i>Bichelelia cincta</i> ^a	MTD	Peduncle	13.4	0.16	0.19	Kang et al. (2011)

ESD, equivalent spherical diameter (μm); μ_{\max} , maximum growth rate (d^{-1}); I_{\max} , maximum ingestion growth rate ($\text{ng C predator}^{-1} \text{ d}^{-1}$); KPD, kleptoplastidic dinoflagellate; MTD, mixotrophic dinoflagellate; HTD, heterotrophic dinoflagellate.

^a μ_{\max} and I_{\max} of the species at a single prey concentration.

^bThe ESD was calculated from the highest cell volume.

^cThe carbon-based unit ($\text{ng C predator}^{-1} \text{ d}^{-1}$) of I_{\max} was converted from the cell-based unit ($\text{cells predator}^{-1} \text{ d}^{-1}$), using the prey size provided in the literature and the regression equation from Strathmann (1967).

^dThe ESD was calculated from the highest cell volume when *Pfiesteria piscicida* fed on *T. amphioxiae*.

Prey	Predator		Shimiella		Karenia		Karlodinium		Takayama	
	gracilenta	RSD	mikimotoi	brevis	armiger	australe	veneficum	helix	tasmanica	
Cyanobacterium										
<i>Synechococcus</i> sp.				O						
Prymnesiophyte										
<i>Chrysotrichomonas</i> sp.	O				O					
<i>Phaeocystis antarctica</i>	O	O	O							
<i>Isochrysis galbana</i>	X		O		O		O	X	X	
Cryptophyte										
<i>Teleaulax amphioxiae</i>	O				O			X	X	
<i>Streptothrix major</i>	O				O		O	X	X	
<i>Rhodomonas salina</i>	O				O	O	O	X	X	
Prasinophyte										
<i>Pyramimonas</i> sp.	O				O					
Chlorophyte										
<i>Dunaliella salina</i>	X									
Dictyochophyte										
<i>Apedinella</i> sp.	O									
<i>Pseudopedinella elastica</i>	X									
Raphidophyte										
<i>Heterosigma akashiwo</i>	X			O				X	X	
Diatom										
<i>Skeletonema costatum</i>	X							X	X	
Dinoflagellate										
<i>Heterocapsa rotundata</i>	X				O			X	X	
<i>Amphidinium carterae</i>	X							X	X	
<i>Effrenium voratum</i>	X				O			X	X	
<i>Procentrum cordatum</i>	X				O			X	X	
<i>Karlodinium veneficum</i>	X				O			O	O	
<i>Heterocapsa steinii</i>	X				O			X	X	
<i>Alexandrium minutum</i>	X				O			O	O	
<i>Karenia mikimotoi</i>	X				O			X	X	
<i>Scrippsiella acuminata</i>	X				O			O	O	
<i>Margalefidinium polykrikoides</i>	X				O			O	O	
<i>Procentrum micans</i>	X				O			X	X	
<i>Akashiwo sanguinea</i>	X				O			X	X	
<i>Tripos furca</i>	X				O					
<i>Alexandrium fraterculus</i>	X				O					
<i>Lingulodinium polyedra</i>	X				O			O	O	
Ciliate										
<i>Mesodinium rubrum</i>	X									
Reference	(1)	(2)	(3)	(4)	(5)	(6)	(7),(8)	(9)	(10)	

Fig. 9. Feeding occurrence by each dinoflagellate predator belonging to the family Kareniaceae on diverse prey species. RSD, the Ross Sea dinoflagellate; O in blue box, feeding; X in red box, no feeding. 1, This study; 2, Sellers et al. (2014); 3, Zhang et al. (2011); 4, Glibert et al. (2009); 5, Berge et al. (2008); 6, de Salas et al. (2005); 7, Li et al. (1999); 8, Yang et al. (2020); 9, Jeong et al. (2016); 10, Lim et al. (2018).

The specific growth rate of *S. gracilenta* SGJH1904 with *T. amphioxiae* filtrate was significantly higher than that with f/2 medium and without any addition. The materials in the prey filtrates were likely to increase the growth rates of *S. gracilenta* SGJH1904. Some phagotrophic dinoflagellates have been reported to utilize dissolved organic materials for their growth (Ou et al. 2014, Hattenrath-Lehmann and Gobler 2015). This evidence suggests that *S. gracilenta* may be able to maintain its abundance using dissolved organic materials released from prey cells.

Many species in the family Kareniaceae, to which *S.*

gracilenta belongs, are known to be mixotrophic or kleptoplastidic dinoflagellates (Li et al. 1999, de Salas et al. 2005, Berge et al. 2008, Glibert et al. 2009, Zhang et al. 2011, Sellers et al. 2014, Jeong et al. 2016, Lim et al. 2018, Yang et al. 2020). Interestingly, the different genera in this family have different prey spectra (Fig. 9): *Takayama* spp. were observed to feed only on dinoflagellates (Jeong et al. 2016, Lim et al. 2018); *Karenia* spp. were observed to feed on a cyanobacterium or prymnesiophyte (Glibert et al. 2009, Zhang et al. 2011); *Karlodinium* spp. feed on diverse prey taxa including prymnesiophytes, cryptophytes, a prasinophyte, a raphidophyte, and dinoflagellates (Li et

al. 1999, de Salas et al. 2005, Berge et al. 2008, Yang et al. 2020). *Shimiella gracilenta* was also observed to feed on various prey taxa, including prymnesiophytes, cryptophytes, a prasinophyte, and a dictyochophyte; however, we did not observe it feeding on dinoflagellates. A possibility that these genera acquired different kleptoplastids from different prey has been suggested (i.e., horizontal gene transfer) (Hehenberger et al. 2019). Thus, differences in the prey spectra among the genera in the family may have led to their generic divergence. Moreover, *S. gracilenta* was able to feed on the prymnesiophyte *P. antarctica* that the Ross Sea dinoflagellate, sister species of *S. gracilenta*, selectively fed on (Sellers et al. 2014). The Ross Sea dinoflagellate was found in the Antarctic region, whereas *S. gracilenta* SGJH1904 was isolated from temperate coastal waters (Gast et al. 2006, Ok et al. 2021a). Therefore, *S. gracilenta* shared the same prey species as sister species, although they lived in largely different regions.

In conclusion, the ecophysiological characteristics of *S. gracilenta* can be summarized as follows: (1) *S. gracilenta* has a wide spatial and temporal distributions in Korean coastal waters; (2) it has the ability to survive in wide ranges of water temperature and salinity, ranging 1.7–26.4°C and 9.9–35.6, respectively; (3) *S. gracilenta* is able to feed on diverse prey species; and (4) it can divide more than twice a day if the optimal prey, *T. amphioxoidea*, is abundant; but (5) it demands approximately 6,000 cells mL⁻¹ of *T. amphioxoidea* as a threshold concentration for growth. Overall, its eurythermal and euryhaline characteristics and the ability to feed on diverse prey species and conduct kleptoplastidy may be responsible for its wide spatial and temporal distributions.

ACKNOWLEDGEMENTS

This research was supported by the National Research Foundation funded by the Ministry of Science and ICT (NRF-2020M3F6A1110582; NRF-2021M3I6A1091272; NRF-2021R1A2C1093379) and by the useful dinoflagellate program of Korea Institute of Marine Science and Technology Promotion (KIMST) funded by the Ministry of Oceans and Fisheries (MOF) award to HJJ.

CONFLICTS OF INTEREST

The authors declare that they have no potential conflicts of interest.

SUPPLEMENTARY MATERIALS

Supplementary Table S1. Sampling date of field samples during 2015–2018 (<https://www.e-algae.org>).

Supplementary Table S2. List of aligned sequences of the internal transcribed spacer region of ribosomal DNA obtained from GenBank to develop the species-specific primers and probe of *Shimiella gracilenta* (<https://www.e-algae.org>).

Supplementary Table S3. List of species used to examine primer and probe specificity for *Shimiella gracilenta* and quantitative real-time polymerase chain reaction results (<https://www.e-algae.org>).

Supplementary Table S4. Taxa and conditions for the isolation of the kleptoplastidic dinoflagellate *Shimiella gracilenta* SGJH1904 and experimental prey organisms used for experiment 1 (<https://www.e-algae.org>).

Supplementary Fig. S1. Standard curve determined by plotting the cycle threshold (Ct) as a function of log (cell abundance) of *Shimiella gracilenta* (<https://www.e-algae.org>).

REFERENCES

- Al-Mutairi, M., Subrahmanyam, M. N. V., Ali, M., Isath, S., AlAwadi, M. A., Kumar, P. N., Al-Hebini, K. & Omar, S. A. S. 2020. Temporal variations in abundance and species richness of phytoplankton with emphasis on diatoms in the subtidal waters of Umm Al-Namil Island, north-western Arabian Gulf of the ROPME Sea Area. *J. Environ. Biol.* 41:1470–1485.
- Back, D. -Y., Ha, S. -Y., Else, B., Hanson, M., Jones, S. F., Shin, K. -H., Tatarek, A., Wiktor, J. M., Cicek, N., Alam, S. & Mundy, C. J. 2021. On the impact of wastewater effluent on phytoplankton in the Arctic coastal zone: a case study in the Kitikmeot Sea of the Canadian Arctic. *Sci. Total Environ.* 764:143861.
- Baek, S. H., Shimode, S., Han, M. -S. & Kikuchi, T. 2008a. Growth of dinoflagellates, *Ceratium furca* and *Ceratium fusus* in Sagami Bay, Japan: the role of nutrients. *Harmful Algae* 7:729–739.
- Baek, S. H., Shimode, S. & Kikuchi, T. 2008b. Growth of dinoflagellates, *Ceratium furca* and *Ceratium fusus* in Sagami Bay, Japan: the role of temperature, light intensity and photoperiod. *Harmful Algae* 7:163–173.
- Berge, T., Hansen, P. J. & Moestrup, Ø. 2008. Feeding mechanism, prey specificity and growth in light and dark of the plastidic dinoflagellate *Karlodinium armiger*. *Aquat. Microb. Ecol.* 50:279–288.

- Bockstahler, K. R. & Coats, D. W. 1993. Spatial and temporal aspects of mixotrophy in Chesapeake Bay dinoflagellates. *J. Eukaryot. Microbiol.* 40:49–60.
- Booth, B. C. & Smith, W. O. Jr. 1997. Autotrophic flagellates and diatoms in the Northeast Water Polynya, Greenland: summer 1993. *J. Mar. Syst.* 10:241–261.
- Burkholder, J. M., Glasgow, H. B. & Deamer-Mella, N. 2001. Overview and present status of the toxic *Pfiesteria* complex (Dinophyceae). *Phycologia* 40:186–214.
- Campbell, P. H. 1973. The phytoplankton of Gales Creek with emphasis on the taxonomy and ecology of estuarine phytoflagellates. Ph.D. dissertation, University of North Carolina, Chapel Hill, NC, USA, 354 pp.
- Cloern, J. E., Alpine, A. E., Cole, B. E., Wong, R. L. J., Arthur, J. F. & Ball, M. D. 1983. River discharge controls phytoplankton dynamics in the northern San Francisco Bay estuary. *Estuar. Coast. Shelf Sci.* 16:415–429.
- Coats, D. W. 1999. Parasitic life styles of marine dinoflagellates. *J. Eukaryot. Microbiol.* 46:402–409.
- Cohu, S., Thibaut, T., Mangialajo, L., Labat, J. -P., Passafiume, O., Blanfuné, A., Simon, N., Cottalorda, J. -M. & Lemée, R. 2011. Occurrence of the toxic dinoflagellate *Ostreopsis cf. ovata* in relation with environmental factors in Monaco (NW Mediterranean). *Mar. Pollut. Bull.* 62:2681–2691.
- Díaz, P., Molinet, C., Cáceres, M. A. & Valle-Levinson, A. 2011. Seasonal and intratidal distribution of *Dinophysis* spp. in a Chilean fjord. *Harmful Algae* 10:155–164.
- Drira, Z., Hamza, A., Belhassen, M., Ayadi, H., Bouaïn, A. & Aleya, L. 2008. Dynamics of dinoflagellates and environmental factors during the summer in the Gulf of Gabes (Tunisia, Eastern Mediterranean Sea). *Sci. Mar.* 72:59–71.
- de Salas, M. F., Bolch, C. J. S. & Hallegraeff, G. M. 2005. *Karlodinium australe* sp. nov. (Gymnodiniales, Dinophyceae), a new potentially ichthyotoxic unarmoured dinoflagellate from lagoonal habitats of south-eastern Australia. *Phycologia* 44:640–650.
- de Sousa, M. I. L. 2020. Biogeography of Arctic Eukaryotic Microbiome: A comparative approach between 18S rRNA gene metabarcoding and microscopic analysis. M.S. dissertation, University of Porto, Porto, Portugal, 94 pp.
- Eom, S. H., Jeong, H. J., Ok, J. H., Park, S. A., Kang, H. C., You, J. H., Lee, S. Y., Yoo, Y. D., Lim, A. S. & Lee, M. J. 2021. Interactions between common heterotrophic protists and the dinoflagellate *Tripos furca*: implication on the long duration of its red tides in the South Sea of Korea in 2020. *Algae* 36:25–36.
- Fraga, S., Rodríguez, E., Bravo, I., Zapata, M. & Marañón, E. 2012. Review of the main ecological features affecting benthic dinoflagellate blooms. *Cryptogam. Algol.* 33:171–179.
- Frost, B. W. 1972. Effects of size and concentration of food particles on the feeding behavior of the marine planktonic copepod *Calanus pacificus*. *Limnol. Oceanogr.* 17:805–815.
- Gast, R. J., Moran, D. M., Beaudoin, D. J., Blythe, J. N., Dennett, M. R. & Caron, D. A. 2006. Abundance of a novel dinoflagellate phylotype in the Ross Sea, Antarctica. *J. Phycol.* 42:233–242.
- Gast, R. J., Moran, D. M., Dennett, M. R. & Caron, D. A. 2007. Kleptoplasty in an Antarctic dinoflagellate: caught in evolutionary transition? *Environ. Microbiol.* 9:39–45.
- Gímez, M. I., Piola, A. R., Kattner, G. & Alder, V. A. 2011. Biomass of autotrophic dinoflagellates under weak vertical stratification and contrasting chlorophyll levels in subantarctic shelf waters. *J. Plankton Res.* 33:1304–1310.
- Glibert, P. M., Burkholder, J. M., Kana, T. M., Alexander, J., Skelton, H. & Shilling, C. 2009. Grazing by *Karenia brevis* on *Synechococcus* enhances its growth rate and may help to sustain blooms. *Aquat. Microb. Ecol.* 55:17–30.
- Golubkov, M., Nikulina, V. & Golubkov, S. 2019. Effects of environmental variables on midsummer dinoflagellate community in the Neva Estuary (Baltic Sea). *Oceanologia* 61:197–207.
- Guillard, R. R. L. & Hargraves, P. E. 1993. *Stichochrysis imobilis* is a diatom, not a chrysophyte. *Phycologia* 32:234–236.
- Guillard, R. R. L. & Ryther, J. H. 1962. Studies of marine planktonic diatoms: I. *Cyclotella nana* Hustedt, and *Detonula confervacea* (Cleve) Gran. *Can. J. Microbiol.* 8:229–239.
- Hallegraeff, G. M. 1993. A review of harmful algal blooms and their apparent global increase. *Phycologia* 32:79–99.
- Hansen, P. J. 1991a. *Dinophysis*: a planktonic dinoflagellate genus which can act both as a prey and a predator of a ciliate. *Mar. Ecol. Prog. Ser.* 69:201–204.
- Hansen, P. J. 1991b. Quantitative importance and trophic role of heterotrophic dinoflagellates in a coastal pelagic food web. *Mar. Ecol. Prog. Ser.* 73:253–261.
- Hattenrath-Lehmann, T. & Gobler, C. J. 2015. The contribution of inorganic and organic nutrients to the growth of a North American isolate of the mixotrophic dinoflagellate, *Dinophysis acuminata*. *Limnol. Oceanogr.* 60:1588–1603.
- Hehenberger, E., Gast, R. J. & Keeling, P. J. 2019. A kleptoplasmidic dinoflagellate and the tipping point between transient and fully integrated plastid endosymbiosis. *Proc. Natl. Acad. Sci.* 116:17934–17942.
- Heinbokel, J. F. 1978. Studies on the functional role of tin-

- tinnids in the Southern California Bight. I. Grazing and growth rates in laboratory cultures. *Mar. Biol.* 47:177–189.
- Hernández-Becerril, D. U., Lau, W. L. S., Hii, K. S., Leaw, C. P., Varona-Cordero, F. & Lim, P. T. 2018. Abundance and distribution of the potentially toxic thecate dinoflagellate *Alexandrium tamarense* (Dinophyceae) in the Central Mexican Pacific, using the quantitative PCR method. *Front. Mar. Sci.* 5:366.
- Jakobsen, H. H., Hansen, P. J. & Larsen, J. 2000. Growth and grazing responses of two chloroplast-retaining dinoflagellates: effect of irradiance and prey species. *Mar. Ecol. Prog. Ser.* 201:121–128.
- Jang, S. H. & Jeong, H. J. 2020. Spatio-temporal distributions of the newly described mixotrophic dinoflagellate *Yihiaella yeosuensis* (Suessiaceae) in Korean coastal waters and its grazing impact on prey populations. *Algae* 35:45–59.
- Jang, S. H., Jeong, H. J., Kwon, J. E. & Lee, K. H. 2017. Mixotrophy in the newly described dinoflagellate *Yihiaella yeosuensis*: a small, fast dinoflagellate predator that grows mixotrophically, but not autotrophically. *Harmful Algae* 62:94–103.
- Jeong, H. J. 1999. The ecological roles of heterotrophic dinoflagellates in marine planktonic community. *J. Eukaryot. Microbiol.* 46:390–396.
- Jeong, H. J., Ha, J. H., Park, J. Y., Kim, J. H., Kang, N. S., Kim, S., Kim, J. S., Yoo, Y. D. & Yih, W. H. 2006. Distribution of the heterotrophic dinoflagellate *Pfiesteria piscicida* in Korean waters and its consumption of mixotrophic dinoflagellates, raphidophytes and fish blood cells. *Aquat. Microb. Ecol.* 44:263–278.
- Jeong, H. J., Ha, J. H., Yoo, Y. D., Park, J. Y., Kim, J. H., Kang, N. S., Kim, T. H., Kim, H. S. & Yih, W. H. 2007. Feeding by the *Pfiesteria*-like heterotrophic dinoflagellate *Luciella masanensis*. *J. Eukaryot. Microbiol.* 54:231–241.
- Jeong, H. J., Kang, H. C., Lim, A. S., Jang, S. H., Lee, K., Lee, S. Y., Ok, J. H., You, J. H., Kim, J. H., Lee, K. H., Park, S. A., Eom, S. H., Yoo, Y. D. & Kim, K. Y. 2021a. Feeding diverse prey as an excellent strategy of mixotrophic dinoflagellates for global dominance. *Sci. Adv.* 7:eabe4214.
- Jeong, H. J., Lee, K. H., Yoo, Y. D., Kang, N. S. & Lee, K. 2011. Feeding by the newly described, nematocyst-bearing heterotrophic dinoflagellate *Gyrodiniellum shiwhaense*. *J. Eukaryot. Microbiol.* 58:511–524.
- Jeong, H. J., Lim, A. S., Franks, P. J. S., Lee, K. H., Kim, J. H., Kang, N. S., Lee, M. J., Jang, S. H., Lee, S. Y., Yoon, E. Y., Park, J. Y., Yoo, Y. D., Seong, K. A., Kwon, J. E. & Jang, T. Y. 2015. A hierarchy of conceptual models of red-tide generation: nutrition, behavior, and biological interactions. *Harmful Algae* 47:97–115.
- Jeong, H. J., Lim, A. S., Yoo, Y. D., Lee, M. J., Lee, K. H., Jang, T. Y. & Lee, K. 2014. Feeding by heterotrophic dinoflagellates and ciliates on the free-living dinoflagellate *Symbiodinium* sp. (Clade E). *J. Eukaryot. Microbiol.* 61:27–41.
- Jeong, H. J., Ok, J. H., Lim, A. S., Kwon, J. E., Kim, S. J. & Lee, S. Y. 2016. Mixotrophy in the phototrophic dinoflagellate *Takayama helix* (family Kareniaceae): predator of diverse toxic and harmful dinoflagellates. *Harmful Algae* 60:92–106.
- Jeong, H. J., Yoo, Y. D., Kang, N. S., Rho, J. R., Seong, K. A., Park, J. W., Nam, G. S. & Yih, W. 2010a. Ecology of *Gymnodinium aureolum*. I. Feeding in western Korean waters. *Aquat. Microb. Ecol.* 59:239–255.
- Jeong, H. J., Yoo, Y. D., Kim, J. S., Kim, T. H., Kim, J. H., Kang, N. S. & Yih, W. 2004. Mixotrophy in the phototrophic harmful alga *Cochlodinium polykrikoides* (Dinophycean): prey species, the effects of prey concentration, and grazing impact. *J. Eukaryot. Microbiol.* 51:563–569.
- Jeong, H. J., Yoo, Y. D., Kim, J. S., Seong, K. A., Kang, N. S. & Kim, T. H. 2010b. Growth, feeding and ecological roles of the mixotrophic and heterotrophic dinoflagellates in marine planktonic food webs. *Ocean Sci. J.* 45:65–91.
- Jeong, H. J., Yoo, Y. D., Lee, K., Kang, H. C., Kim, J. S. & Kim, K. Y. 2021b. Annual carbon retention of a marine-plankton community in the eutrophic Masan Bay, based on daily measurements. *Mar. Biol.* 168:69.
- Jeong, H. J., Yoo, Y. D., Lee, K. H., Kim, T. H., Seong, K. A., Kang, N. S., Lee, S. Y., Kim, J. S., Kim, S. & Yih, W. H. 2013. Red tides in Masan Bay, Korea in 2004–2005: I. Daily variations in the abundance of red-tide organisms and environmental factors. *Harmful Algae* 30(Suppl. 1):S75–S88.
- Jeong, H. J., Yoo, Y. D., Park, J. Y., Song, J. Y., Kim, S. T., Lee, S. H., Kim, K. W. & Yih, W. H. 2005a. Feeding by phototrophic red-tide dinoflagellates: five species newly revealed and six species previously known to be mixotrophic. *Aquat. Microb. Ecol.* 40:133–150.
- Jeong, H. J., Yoo, Y. D., Seong, K. A., Kim, J. H., Park, J. Y., Kim, S. H., Lee, S. H., Ha, J. H. & Yih, W. H. 2005b. Feeding by the mixotrophic dinoflagellate *Gonyaulax polygramma*: mechanisms, prey species, effects of prey concentration, and grazing impact. *Aquat. Microb. Ecol.* 38:249–257.
- Johnson, M. D. 2011. The acquisition of phototrophy: adaptive strategies of hosting endosymbionts and organelles. *Photosynth. Res.* 107:117–132.
- Johnson, M. D., Stoecker, D. K. & Marshall, H. G. 2013. Seasonal dynamics of *Mesodinium rubrum* in Chesapeake Bay. *J. Plankton Res.* 35:877–893.
- Kang, H. C., Jeong, H. J., Lim, A. S., Ok, J. H., You, J. H., Park, S. A., Lee, S. Y. & Eom, S. H. 2020. Effects of temperature on

- the growth and ingestion rates of the newly described mixotrophic dinoflagellate *Yiharella yeosuensis* and its two optimal prey species. *Algae* 35:263–275.
- Kang, H. C., Jeong, H. J., Ok, J. H., You, J. H., Jang, S. H., Lee, S. Y., Lee, K. H., Park, J. Y. & Rho, J. -R. 2019. Spatial and seasonal distributions of the phototrophic dinoflagellate *Biecheleriopsis adriatica* (Suessiaceae) in Korea: quantification using qPCR. *Algae* 34:111–126.
- Kang, N. S., Jeong, H. J., Yoo, Y. D., Yoon, E. Y., Lee, K. H., Lee, K. & Kim, G. 2011. Mixotrophy in the newly described phototrophic dinoflagellate *Woloszynskia cincta* from western Korean waters: feeding mechanism, prey species and effect of prey concentration. *J. Eukaryot. Microbiol.* 58:152–170.
- Kibbe, W. A. 2007. OligoCalc: an online oligonucleotide properties calculator. *Nucleic Acids Res.* 35:W43–W46.
- Kim, J. S., Jeong, H. J., Yoo, Y. D., Kang, N. S., Kim, S. K., Song, J. Y., Lee, M. J., Kim, S. T., Kang, J. H., Seong, K. A. & Yih, W. H. 2013. Red tides in Masan Bay, Korea, in 2004–2005: III. Daily variations in the abundance of mesozooplankton and their grazing impacts on red-tide organisms. *Harmful Algae* 30(Suppl. 1):S102–S113.
- Larsen, J. 1988. An ultrastructural study of *Amphidinium poecilochroum* (Dinophyceae), a phagotrophic dinoflagellate feeding on small species of cryptophytes. *Phycologia* 27:366–377.
- Larsen, J. 1994. Unarmoured dinoflagellates from Australian waters I. The genus *Gymnodinium* (Gymnodiniales, Dinophyceae). *Phycologia* 33:24–33.
- Lee, K. H., Jeong, H. J., Kang, H. C., Ok, J. H., You, J. H. & Park, S. A. 2019a. Growth rates and nitrate uptake of co-occurring red-tide dinoflagellates *Alexandrium affine* and *A. fraterculus* as a function of nitrate concentration under light-dark and continuous light conditions. *Algae* 34:237–251.
- Lee, K. H., Jeong, H. J., Kwon, J. E., Kang, H. C., Kim, J. H., Jang, S. H., Park, J. Y., Yoon, E. Y. & Kim, J. S. 2016. Mixotrophic ability of the phototrophic dinoflagellates *Alexandrium andersonii*, *A. affine*, and *A. fraterculus*. *Harmful Algae* 59:67–81.
- Lee, S. Y., Jeong, H. J., Kang, H. C., Ok, J. H., You, J. H., Park, S. A. & Eom, S. H. 2021. Comparison of the spatial-temporal distributions of the heterotrophic dinoflagellates *Gyrodinium dominans*, *G. jinhaense*, and *G. moestrupii* in Korean coastal waters. *Algae* 36:37–50.
- Lee, S. Y., Jeong, H. J., Kwon, J. E., You, J. H., Kim, S. J., Ok, J. H., Kang, H. C. & Park, J. Y. 2019b. First report of the photosynthetic dinoflagellate *Heterocapsa minima* in the Pacific Ocean: morphological and genetic characterizations and the nationwide distribution in Korea. *Algae* 34:7–21.
- Lee, S. Y., Jeong, H. J., Ok, J. H., Kang, H. C. & You, J. H. 2020. Spatial-temporal distributions of the newly described mixotrophic dinoflagellate *Gymnodinium smaydae* in Korean coastal waters. *Algae* 35:225–236.
- Li, A., Stoecker, D. K. & Adolf, J. E. 1999. Feeding, pigmentation, photosynthesis and growth of the mixotrophic dinoflagellate *Gyrodinium galatheanum*. *Aquat. Microb. Ecol.* 19:163–176.
- Li, A., Stoecker, D. K. & Coats, D. W. 2000. Spatial and temporal aspects of *Gyrodinium galatheanum* in Chesapeake Bay: distribution and mixotrophy. *J. Plankton Res.* 22:2105–2124.
- Lim, A. S., Jeong, H. J., Ok, J. H. & Kim, S. J. 2018. Feeding by the harmful phototrophic dinoflagellate *Takayama tasmanica* (Family Kareniaceae). *Harmful Algae* 74:19–29.
- Lin, S., Zhang, H. & Dubois, A. 2006. Low abundance distribution of *Pfiesteria piscicida* in Pacific and Western Atlantic as detected by mtDNA-18S rDNA real-time polymerase chain reaction. *J. Plankton Res.* 28:667–681.
- Litaker, R. W., Vandersea, M. W., Kibler, S. R., Reece, K. S., Stokes, N. A., Steidinger, K. A., Millie, D. F., Bendis, B. J., Pigg, R. J. & Tester, P. A. 2003. Identification of *Pfiesteria piscicida* (Dinophyceae) and *Pfiesteria*-like organisms using internal transcribed spacer-specific PCR assays. *J. Phycol.* 39:754–761.
- Martin, J. R. & Gypens, N. 2021. Temperate waters: NCM succession and spatial variability in The North Sea revealed by DNA metabarcoding. In Mitra, A., Hansen, P. J. & Flynn, K. J. (Eds.) *Report of Seasonal Distribution of Non-constitutive Mixoplankton across Arctic, Temperate and Mediterranean Coastal Waters*. Zenodo, pp. 21–30.
- Mathot, S., Smith, W. O. Jr., Carlson, C. A., Garrison, D. L., Gowing, M. M. & Vickers, C. L. 2000. Carbon partitioning within *Phaeocystis antarctica* (Prymnesiophyceae) colonies in the Ross Sea, Antarctica. *J. Phycol.* 36:1049–1056.
- Matsubara, T., Nagasoe, S., Yamasaki, Y., Shikata, T., Shimasaki, Y., Oshima, Y. & Honjo, T. 2007. Effects of temperature, salinity, and irradiance on the growth of the dinoflagellate *Akashiwo sanguinea*. *J. Exp. Mar. Biol. Ecol.* 342:226–230.
- Ok, J. H., Jeong, H. J., Lee, S. Y., Park, S. A. & Noh, J. H. 2021a. *Shimiella* gen. nov. and *Shimiella gracilenta* sp. nov. (Dinophyceae, Kareniaceae), a kleptoplastidic dinoflagellate from Korean waters and its survival under starvation. *J. Phycol.* 57:70–91.
- Ok, J. H., Jeong, H. J., Lim, A. S. & Lee, K. H. 2017. Interactions between the mixotrophic dinoflagellate *Takayama helix* and common heterotrophic protists. *Harmful Algae* 68:178–191.

- Ok, J. H., Jeong, H. J., Lim, A. S., You, J. H., Kang, H. C., Kim, S. J. & Lee, S. Y. 2019. Effects of light and temperature on the growth of *Takayama helix* (Dinophyceae): mixotrophy as a survival strategy against photoinhibition. *J. Phycol.* 55:1181–1195.
- Ok, J. H., Jeong, H. J., You, J. H., Kang, H. C., Park, S. A., Lim, A. S., Lee, S. Y. & Eom, S. H. 2021b. Phytoplankton bloom dynamics in incubated natural seawater: predicting bloom magnitude and timing. *Front. Mar. Sci.* 8:681252.
- Ou, L., Lundgren, V., Lu, S. & Granéli, E. 2014. The effect of riverine dissolved organic matter and other nitrogen forms on the growth and physiology of the dinoflagellate *Prorocentrum minimum* (Pavillard) Schiller. *J. Sea Res.* 85:499–507.
- Park, S. A., Jeong, H. J., Ok, J. H., Kang, H. C., You, J. H., Eom, S. H. & Park, E. C. 2021. Interactions between the kleptoplastidic dinoflagellate *Shimiella gracilenta* and several common heterotrophic protists. *Front. Mar. Sci.* 8:738547.
- Peterson, D. H. & Festa, J. F. 1984. Numerical simulation of phytoplankton productivity in partially mixed estuaries. *Estuar. Coast. Shelf Sci.* 19:563–589.
- Raven, J. A., Beardall, J., Flynn, K. J. & Maberly, S. C. 2009. Phagotrophy in the origins of photosynthesis in eukaryotes and as a complementary mode of nutrition in phototrophs: relation to Darwin's insectivorous plants. *J. Exp. Bot.* 60:3975–3987.
- Schnepf, E. 1992. From prey via endosymbiont to plastid: comparative studies in dinoflagellates. In Lewin, R. A. (Ed.) *Origins of Plastids: Symbiogenesis, Prochlorophytes, and the Origins of Chloroplasts*. Springer, Boston, MA, pp. 53–76.
- Schnepf, E. & Elbrächter, M. 1992. Nutritional strategies in dinoflagellates: a review with emphasis on cell biological aspects. *Eur. J. Protistol.* 28:3–24.
- Schnepf, E. & Elbrächter, M. 1999. Dinophyte chloroplasts and phylogeny: a review. *Grana* 38:81–97.
- Sellers, C. G., Gast, R. J. & Sanders, R. W. 2014. Selective feeding and foreign plastid retention in an antarctic dinoflagellate. *J. Phycol.* 50:1081–1088.
- Skovgaard, A. 1998. Role of chloroplast retention in a marine dinoflagellate. *Aquat. Microb. Ecol.* 15:293–301.
- Smalley, G. W. & Coats, D. W. 2002. Ecology of the red-tide dinoflagellate *Ceratium furca*: distribution, mixotrophy, and grazing impact on ciliate populations of Chesapeake Bay. *J. Eukaryot. Microbiol.* 49:63–73.
- Smayda, T. J. & Reynolds, C. S. 2003. Strategies of marine dinoflagellate survival and some rules of assembly. *J. Sea Res.* 49:95–106.
- Stat, M., Morris, E. & Gates, R. D. 2008. Functional diversity in coral–dinoflagellate symbiosis. *Proc. Natl. Acad. Sci. U. S. A.* 105:9256–9261.
- Stoecker, D. K., Hansen, P. J., Caron, D. A. & Mitra, A. 2017. Mixotrophy in the marine plankton. *Annu. Rev. Mar. Sci.* 9:311–335.
- Strathmann, R. R. 1967. Estimating the organic carbon content of phytoplankton from cell volume or plasma volume. *Limnol. Oceanogr.* 12:411–418.
- Tamura, K., Dudley, J., Nei, M. & Kumar, S. 2007. MEGA4: molecular evolutionary genetics analysis (MEGA) software version 4.0. *Mol. Biol. Evol.* 24:1596–1599.
- Taylor, F. J. R., Hoppenrath, M. & Saldarriaga, J. F. 2008. Dinoflagellate diversity and distribution. *Biodivers. Conserv.* 17:407–418.
- Tillmann, U. & Reckermann, M. 2002. Dinoflagellate grazing on the raphidophyte *Fibrocapsa japonica*. *Aquat. Microb. Ecol.* 26:247–257.
- Unrein, F., Gasol, J. M., Not, F., Forn, I. & Massana, R. 2014. Mixotrophic haptophytes are key bacterial grazers in oligotrophic coastal waters. *ISME J.* 8:164–176.
- Verity, P. G., Stoecker, D. K., Sieracki, M. E., Burkill, P. H., Edwards, E. S. & Tronzo, C. R. 1993. Abundance, biomass and distribution of heterotrophic dinoflagellates during the North Atlantic spring bloom. *Deep Sea Res. II Top. Stud. Oceanogr.* 40:227–244.
- Yang, H., Hu, Z., Shang, L., Deng, Y. & Tang, Y. Z. 2020. A strain of the toxic dinoflagellate *Karlodinium veneficum* isolated from the East China Sea is an omnivorous phagotroph. *Harmful Algae* 93:101775.
- Yoo, Y. D., Jeong, H. J., Kang, N. S., Song, J. Y., Kim, K. Y., Lee, G. & Kim, J. 2010. Feeding by the newly described mixotrophic dinoflagellate *Paragymnodinium shiwhaense*: feeding mechanism, prey species, and effect of prey concentration. *J. Eukaryot. Microbiol.* 57:145–158.
- Yoo, Y. D., Jeong, H. J., Kim, J. S., Kim, T. H., Kim, J. H., Seong, K. A., Lee, S. H., Kang, N. S., Park, J. W., Park, J., Yoon, E. Y. & Yih, W. H. 2013. Red tides in Masan Bay, Korea in 2004–2005: II. Daily variations in the abundance of heterotrophic protists and their grazing impact on red-tide organisms. *Harmful Algae* 30(Suppl. 1):S89–S101.
- You, J. H., Jeong, H. J., Kang, H. C., Ok, J. H., Park, S. A., & Lim, A. S. 2020. Feeding by common heterotrophic protist predators on seven *Prorocentrum* species. *Algae* 35:61–78.
- Zhang, Q., Yu, R., Song, J., Yan, T., Wang, Y. & Zhou, M. 2011. Will harmful dinoflagellate *Karenia mikimotoi* grow phagotrophically? *Chin. J. Oceanol. Limnol.* 29:849–859.